RADC-TDR-63-406

September 1963

FINAL REPORT

INTERFERENCE MONITOR FEASIBILITY STUDY

(PHASE III)

RADIATION INCORPORATED
MELBOURNE, FLORIDA

CONTRACTORS REPORT NO. 1593-3

CONTRACT NO. AF 30(602)2695

PREPARED FOR

ROME AIR DEVELOPMENT CENTER

AIR RESEARCH AND DEVELOPMENT COMMAND

UNITED STATES AIR FORCE

GRIFFISS AIR FORCE BASE

NEW YORK

RADIATION
Melbourne
A Division of Radiation Incorporated

APPROPRIATE NOTICES: Qualified requestors may obtain copies from ASTIA. Orders will be expedited if placed through the librarian or other person designated to request documents from ASTIA.

LEGAL NOTICES:

When U.S. Government drawings, specifications or other data are used for any purpose other than a definitely related government procurement operation, the government thereby incurs no responsibility nor any obligation whatsoever, and the fact that the government may have formulated, furnished, or in any way supplied the said drawings, specifications, or other data is not to be regarded by implication or otherwise, as in any manner licensing the holder or any other person or corporation or conveying any rights or permission to manufacture, use or sell any patented invention that may in any way be related thereto

DISPOSITION NOTICE:

Do not return this copy. Retain or destroy.

RADC-TDR-63-406

September 1963

FINAL REPORT

INTERFERENCE MONITOR FEASIBILITY STUDY

(PHASE III)

RADIATION INCORPORATED
MELBOURNE, FLORIDA

CONTRACTORS REPORT NO. 1593-3

CONTRACT NO. AF 30(602)2695

PREPARED FOR

ROME AIR DEVELOPMENT CENTER

AIR RESEARCH AND DEVELOPMENT COMMAND

UNITED STATES AIR FORCE

GRIFFISS AIR FORCE BASE

NEW YORK

FOREWORD

The study and investigation reported in this report have been supported by the Applied Research Branch of the Rome Air Development Center, Griffiss Air Force Base under contract AF 30(602)-2695. The study is included in Project 4540, Task 454001 under the direction of:

Louis F. Moses
Task Engineer
Applied Research Branch, and

John L. Elberson
Program Monitor
Applied Research Branch

The following contractor personnel contributed to the investigations and this report:

G. Duggan

W. F. Quinlivan

K. M. Wooded

ABSTRACT

The design of the feasibility breadboard model RFI monitor has been completed and the laboratory test results are presented. An on site feasibility demonstration was conducted at the Verona Test Site by Radiation personnel with RAUMA participation. The recorded results of the field demonstration are presented.

Recommendations are made concerning the philosophy, specifications, and implementation of an ultimate RFI monitor.

PUBLICATION REVIEW

This report has been reviewed and is approved. For further technical information on this project, contact Mr. Louis F. Moses, RAUMA, Ext. 7641.

Louis F. Moses

Approved: LOUIS F. MOSES
Project Engineer
Applied Research Branch

Samuel D. Zaccari

Approved: SAMUEL D. ZACCARI, Chief
Electromagnetic Vulnerability Lab
Directorate of Communications

FOR THE COMMANDER: Fred J. Diamond
for IRVING J. GABELMAN
Director of Advanced Studies

TABLE OF CONTENTS

LIST OF ILLUSTRATIONS

1.0 INTRODUCTION

The Interference Monitor Feasibility Program is a study for the purpose of developing techniques for the continuous monitoring of the spectrum radiated by pulse radar transmitters. Techniques have been sought which permit recording only when the levels of peak effective radiated power exceed the values specified in paragraph 3.5 of MIL-R-27055 (USAF).

1.1 Objective of the Program

The objective of this program is to define the problems in monitoring the spectrum from 200 mc to 40 Gc and to investigate possible technical approaches to implement a solution.

1.2 Previous Work

The first Technical Note, RADC-TDR-62-505, covered the work on the program to 20 August 1962. Effort ta that time consisted of a study in the areas of defining the expected spectral characteristics, determining the factors to be considered in locating the monitor, and assimilating and organizing other information relative to RF component availability and performance.

The second Technical Note, RADC-TDR-63-198 covered the work of the program to 15 March 1963. Effort consisted mainly of defining the technical approach in terms of hardware and implementing a breadboard model ta demonstrate the feasibility of the selected monitor approach.

1.3 Scope of this Report

To meet the objectives of the program, a breadboard monitor, operating from 2 Gc to 4 Gc has been constructed and utilized to demonstrate the feasibility of the recommended monitor technique. This report covers the design completion of the feasibility breadboard model and contains a synthesis of recorded results of RFI testing in both the laboratory and the field. Recommendations for the ultimate monitor design are made at the conclusion of this report.

2.0 FEASIBILITY BREADBOARD

2.1 Breadboard Design Completion

A number of design changes have accumulated in the breadboard monitor since the release of Technical Note 2, all of which occur in the circuitry following the balanced mixer. Hence, a block diagram of this portion of the system appears in Figure 1 for discussion. The decision favoring a 30 mc IF over a zero IF presents problems in dynamic range brought on by impedance considerations. As assumed in Technical Note 2 (pages 48 and 49), the threshold network is driven from a low impedance source to minimize charge time of the capacitor in the peak detector. However, terminating the 30 mc IF amplifier with a 50 ohm resistance to yield a low equivalent output impedance has the deleterious effect of limiting the maximum output amplitude and hence the dynamic range of the amplifier in addition to reducing its gain. To avoid this problem in the breadboard, a buffer consisting of a pre-detector and video amplifier was added between the 30 mc IF

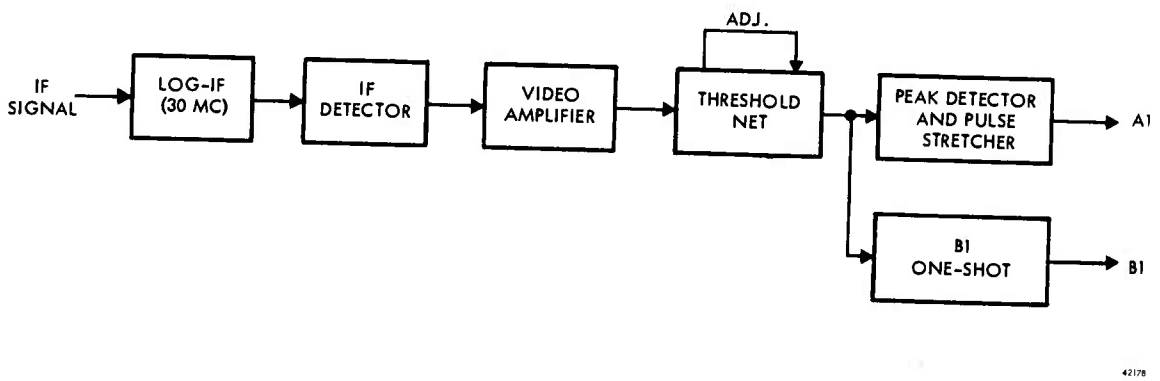

Figure 1. Block Diagram of Subsystem Following Balanced Mixer

amplifier and the threshold network. By using a pre-detector, the value of capacitance in the detectar may be chosen compatible with the output resistance of the IF amplifier (1K) withaut resarting to a 50 ohm termination. The input resistance of the video amplifier shunts the detector capacitor to a time constant that reproduces the RF pulse envelope. The emitter follower output of the videa amplifier yields a low autput impedance for driving the threshold network as required.

An eight stage 30 mc IF amplifier was modified for the breadboard monitar to produce a quasi-logarithmic transfer function to achieve greater dynamic range. A plot of the input-output curve appears in Figure 3. The logarithmic behavior (output voltage linear to input power in db) Is obtained through use of parallel back-to-back germanimum diodes as shown schematically in Figure 2. The volt-ampere curve of a germanimum diode is approximately logarithmic. That is, the voltage across the diade is proportional to the logarithm of the current through it. In case of interest, the diodes are driven from an approximate current source. Hence, the transfer function is logarithmic. Some of the peculiarities of this logarithmic amplifier as it affects bandwidth and resonance are shown in the curves of Figure 4. The bandwidth and resonance point are both functions of input signal level as indicated.

Following the IF detector is a video amplifier, the circuit diagram of which appears in Figure 5. It has a gain of 2.5, an input impedance of 1 kilohm, and an output impedance less than 1 ohm for signals with a pulse width

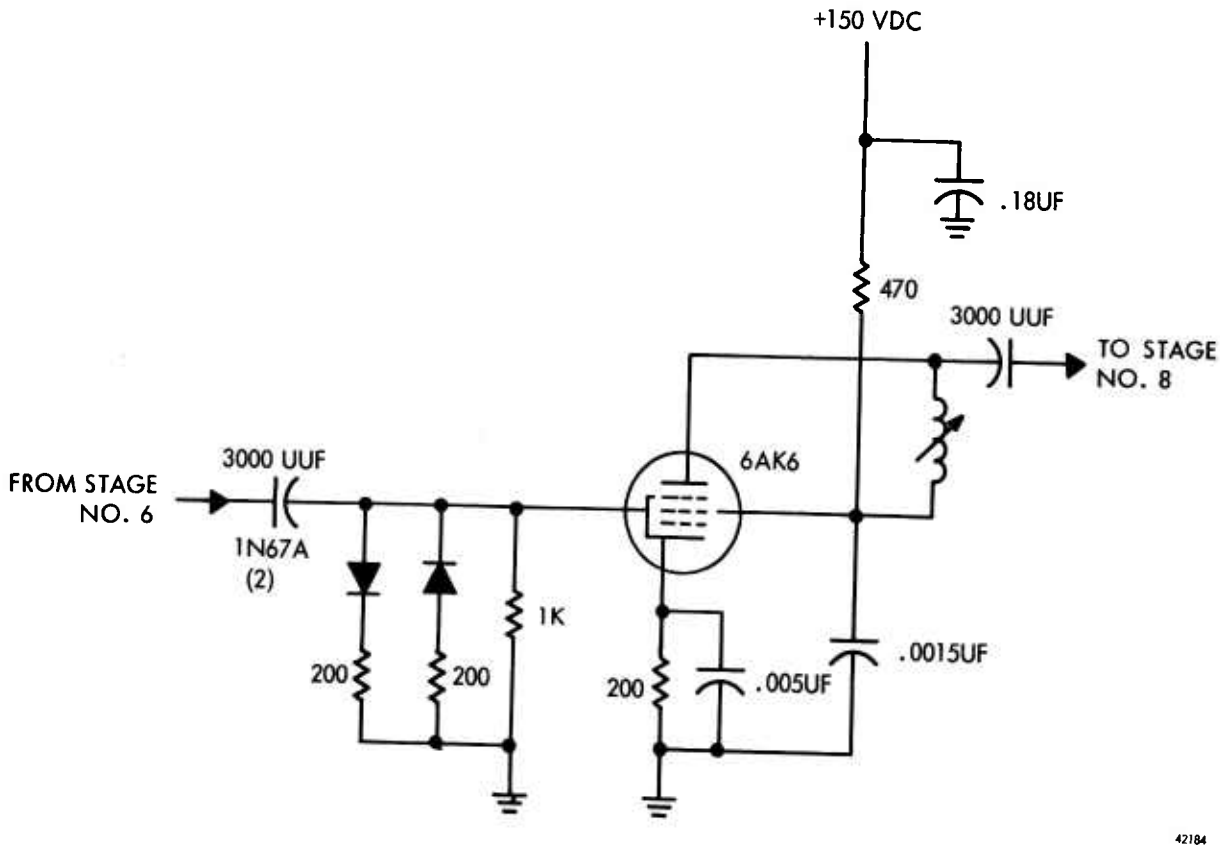

Figure 2. Schematic - 30 mc Log IF, Stage 7

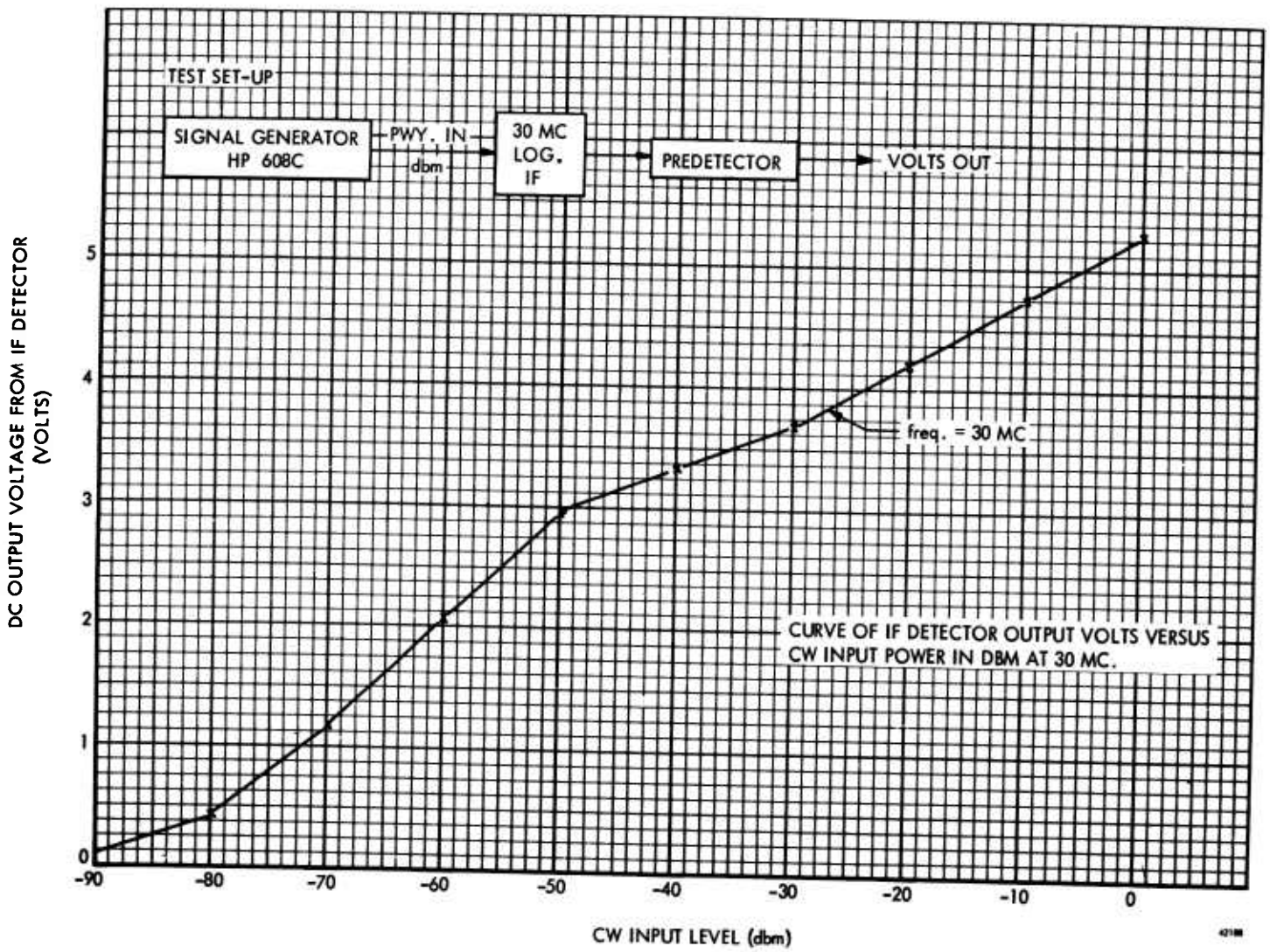

Figure 3. Curve - IF Detector Output Volts vs Input Power

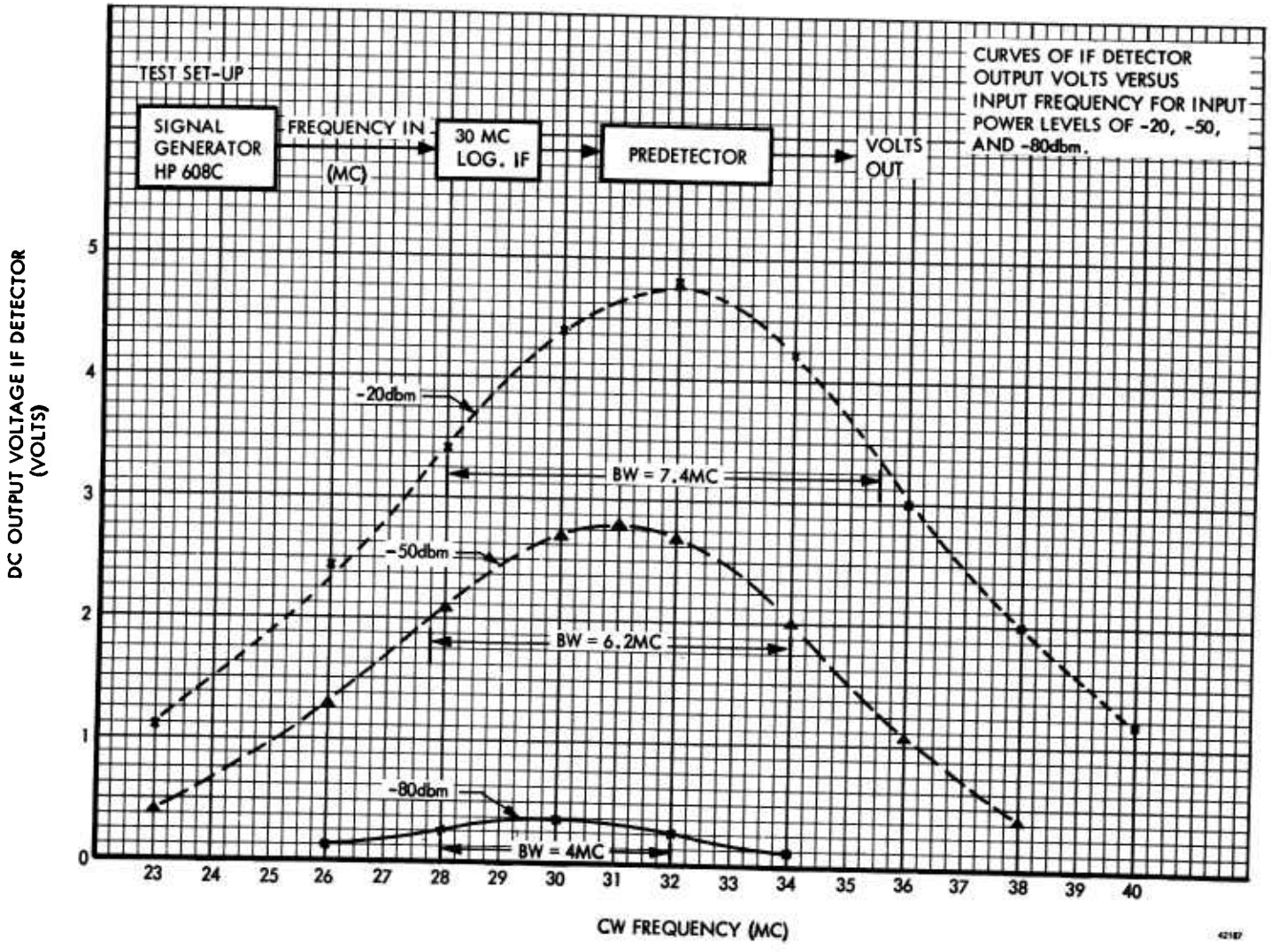

Figure 4. Curve - IF Detector Output Volts vs Frequency

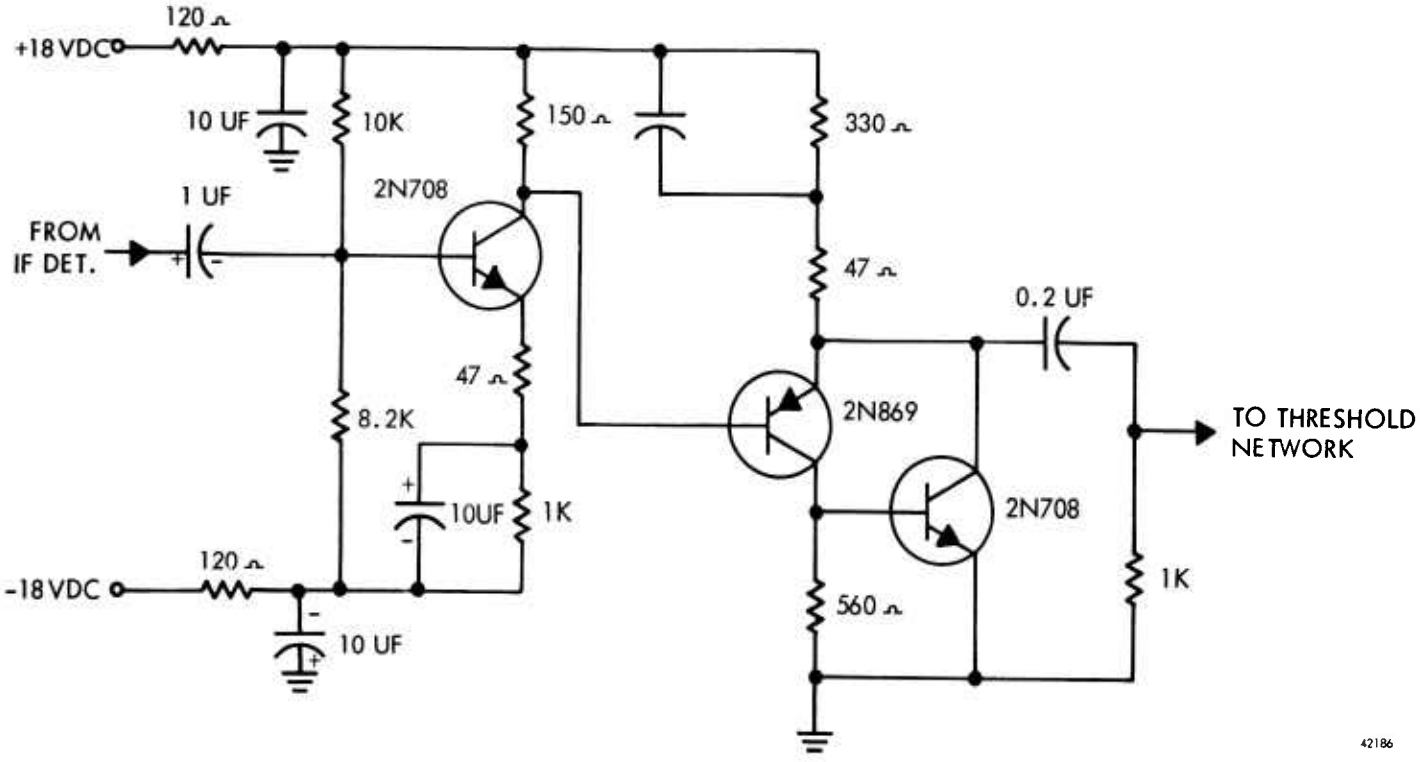

Figure 5. Schematic - Video Amplifier

between 0.2 and 20 micro-seconds. The low output impedance is obtained through use of a complementary (PNP-NPN) compound-connected emitter follower output stage.

2.2 Breadboard Laboratory Test Results

To evaluate the breadboard monitor as a system, a series of tests were conducted in the lab to simulate conditions expected at the Verona test site. A block diagram of the test set-up appears in Figure 6. Two S band signal generators (HP 616B) having calibrated attenuators are used to simulate radar transmitters. Both signals are coupled to the TWT input of the monitor through a power divider. Signal generator A simulates the radar having a coaxial cable connection to provide pre-trigger pulses at the Verona test site. Hence the sync output (pre-trigger) of pulse generator is connected to the identification block in the monitor and the delayed output (mainbang) is connected to the sync input signal generator A. To demonstrate the effect of gating the TWT to reduce or eliminate unwanted signals, pulse generator 2 synchronizes signal generator B. The pulse generator main output is connected to the gate input of the TWT so that when aligned properly (pulse width and delay) the gate pulse overlaps in time the mainbang RF pulse emanating from signal generator B. A dual channel Sanborne Chart Recorder (Model 320) is used to record the interference amplitude on one channel and the identification pulses on the other channel. A review of results follows:

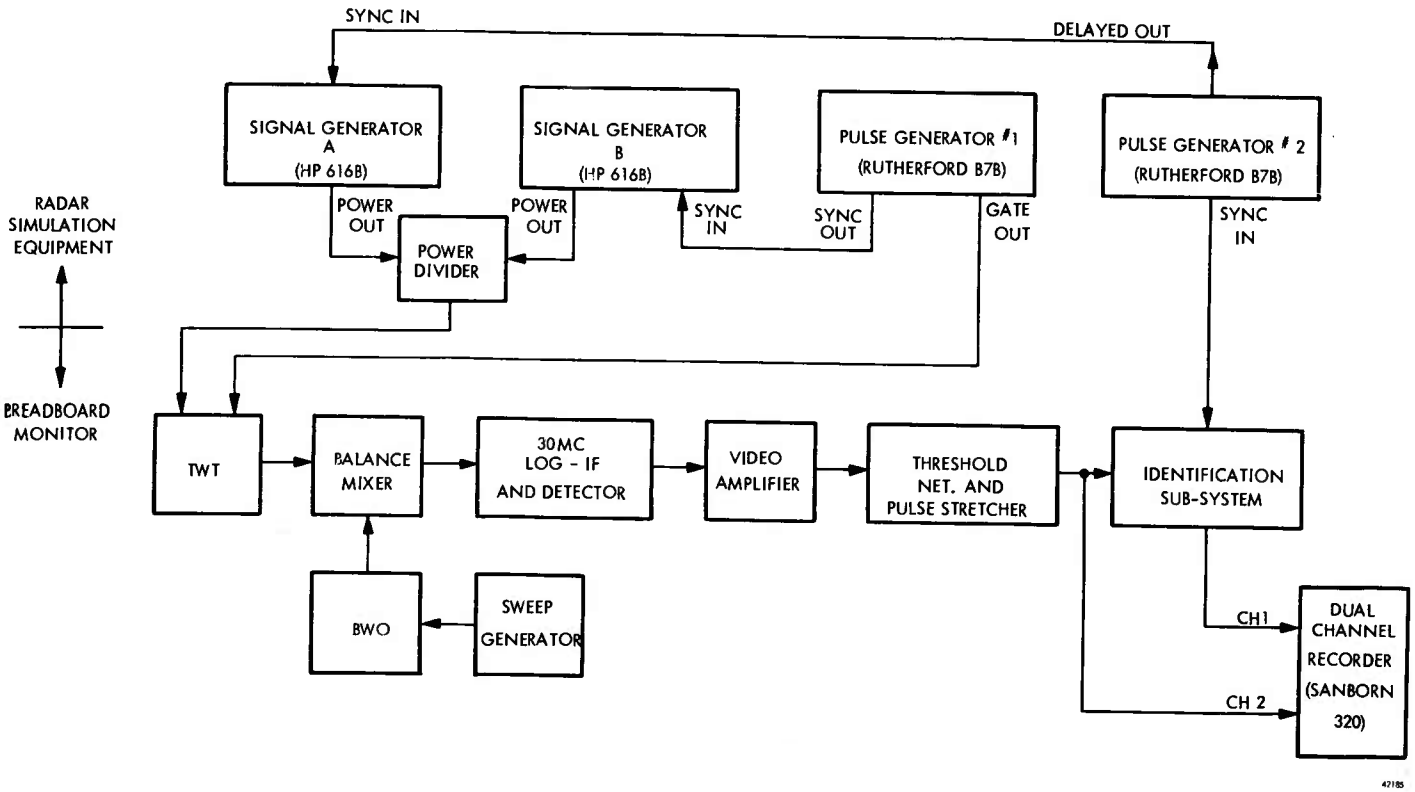

Figure 6. Laboratory Test Set-up

2.2.1 Test I

2.2.1.1 Objectives

1. To record signal amplitude and identify the source.

2. To show the effect of signal overload on the system response.

2.2.1.2 Conditions

The test set-up is shown in Figure 6 except that signal generator B is turned off. Signal generator A conditions:

RF Frequency	-3 KMC
Pulse repetition frequency	-2 KC
Pulse width	-10 micro-sec.
Recorder Speed	-5 mm/sec.

2.2.1.3 Results*

Figure 7a is a recording of the monitor response to the 3 KMC signal coming from signal generator A at a power level of -65 dbm. The source identification of the signal is shown in the channel directly above the response. If the first response peak is called the signal, then the second response peak may be considered its image. Hence, every recorded signal appears as a double response separated by twice the IF center frequency, 60 mc. The absolute frequency of the signal (3 KMC) lies midway between the two response peaks and is determined by calibrating the time scale in

* On all recordings in this section the top channel is identification and the bottom channel is signal amplitude.

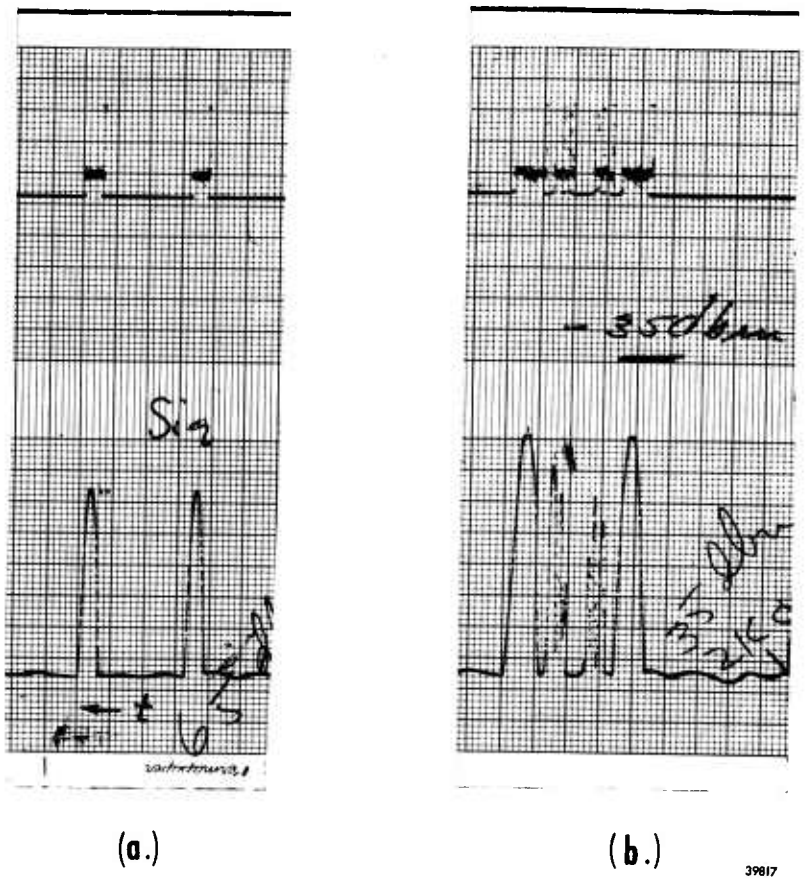

Figure 7. Oscillographs - Test I

terms of frequency with frequency markers (not shown).

Figure 7b illustrates the effect of system overload caused by increasing the output power level of signal generator A to -35 dbm. At first glance it appears that another RF signal is present between the outside peaks. The identification, however, signifies that the entire response is caused by generator A. As determined by experiment, this phenomena is caused by sub-multiples of the 30 mc IF frequency entering the IF amplifier input from the balanced mixer. To illustrate, when the BWO frequency is within 15 mc of the signal frequency, a difference of 15 mc is produced at the output of the mixer. Due to insufficient skirts on the 30 mc bandpass filter of the first stage of the IF amplifier, some of the 15 mc signal impinges on the diodes used to produce logarithmic characteristics of the amplifier. When the 15 mc level is large enough to switch the diodes, multiples of 15 mc are produced, and any 30 mc per second harmonic signals are amplified by the succeeding stages. Similarly, a 10 mc difference frequency from the mixer is trebled by the diodes likewise producing a 30 mc signal and so on. A whole series of psuedo-interference signals are thus generated, the visibility of which is a function of signal strength. Close inspection of Figure 7B reveals three distinct peaks (not including the image response) in addition to the true peak, caused by multiplication of the 7.5, 10 and 15 mc IF difference frequencies generated at the mixer output during the sweep. This effect can be eliminated in the ultimate monitor by including a sharp skirted 30 mc bandpass filter in the first stage of the IF amplifier.

2.2.2 Test II

2.2.2.1 Objectives

1. To display the response of two distinct RF signals on the recorder and the means of identifying one from the other.

2. To show the effect of a random false identification.

2.2.2.2 Conditions

The test set-up is shown in Figure 6 with signal generators A and B both operating but TWT blanking gate off.

Signal Generator A:

RF Signal level	-75 dbm
RF frequency	3 KMC
Pulse repetition frequency	300 cps
Pulse width	10 micro-sec.

Signal Generator B:

RF frequency	3.1, 3.03 KMC
Pulse Repetition frequency	300 cps
Pulse width	10 micro-sec.

2.2.2.3 Results

Figure 8a is a recording of the monitor response to two distinct RF signals; one from generator A, the other from generator B. The frequency

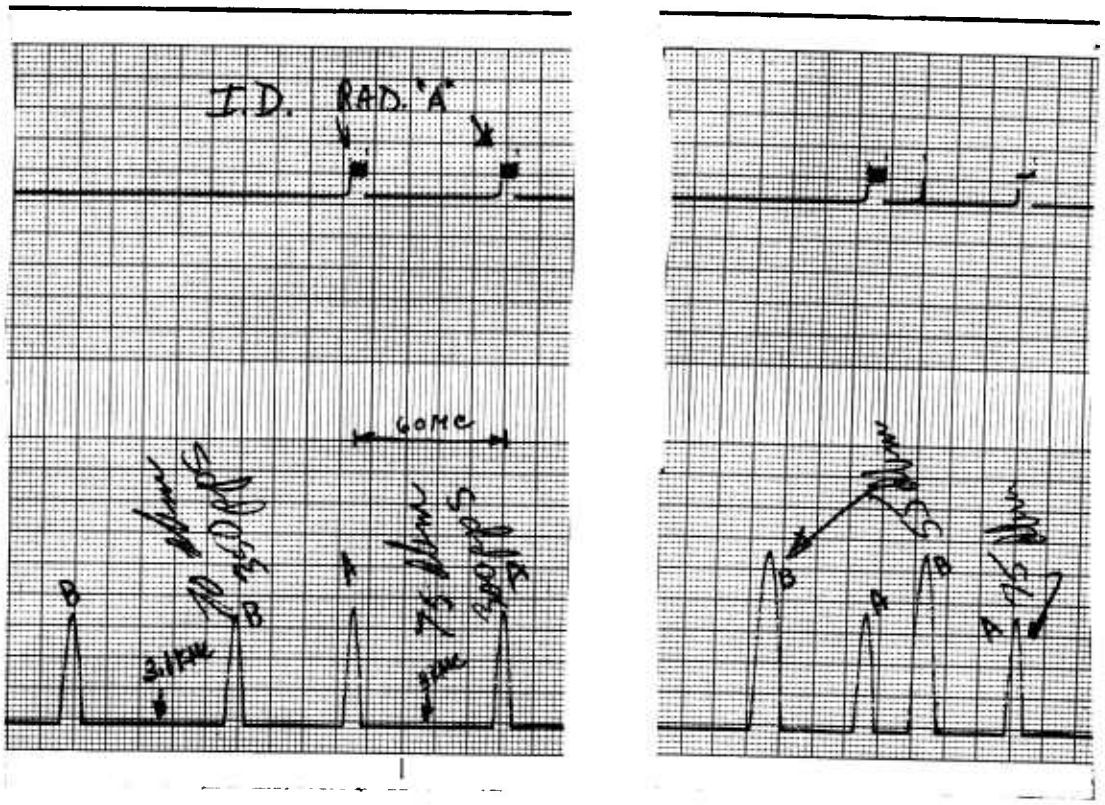

(a.) (b.)

39818

Figure 8. Oscillographs - Test II

of B is pre-set to 3.1 KMC. The identification system is set up to identify A. Hence, identification pulses appear on the display directly above the response of generator A. Figure 8b represents a similar recording except that the signal level and frequency of generator B is changed to -55 dbm and 3.03 KMC respectively. A significant observation is that a false identification pulse appears directly above one of the B response peaks. This occurs because of a random porcess in which the "on time" of generator B is time coincident with the "on time" of generator A. Note, however, that the false identification only lasts for a short time relative to the width of the B response as opposed to the true identification which lasts for the entire A response time interval. Hence, in this case, there is no practical problem in distinguishing the true identification from the false. In a situation where many signals are present and identification based on pulse amplitude is assigned to each signal, false identification would be a serious problem. For this reason, a modification to the identification system for the ultimate monitor is proposed at the end of this report to eliminate false identifications.

2.2.3 Test III

The objective of this test was to show the feasibility of gating the TWT to eliminate an unwanted signal.

2.2.3.1 Conditions

The test set-up is shown in Figure 6 with signal generators A and B both operating. For the first part of the test, the TWT blanking gate is off, for

the second part of the test it is on.

Signal Generator A:	Same conditions as Test II
Signal Generator B:	
RF signal level	-35 dbm
RF frequency	3 KMC
Pulse rate	300 cps
Pulse width	10 micro-sec.

2.2.3.2 Results

Figure 9a is a recording of the monitor response to two distinct RF signals, A and B. Signal B is considerably larger (40 db) than A and its frequency is nearly the same. This produces a response in which the effects of B wash out the effects of A. Note that the signal strength of B is sufficient to produce a psuedo-interference signal corresponding to a difference frequency of 15 mc. Figure 9b is a recording under exactly the same conditions except that a blanking gate pulse is applied to the TWT, time coincident with RF signal B. Signal B is thus eliminated from the display yielding the response of signal A.

2.3 Breadboard Field Tests

2.3.1 Purpose of Field Tests

In accordance with the requirement set forth in Exhibit A of contract AF 30(602)-2695, an S band feasibility breadboard monitor was shipped

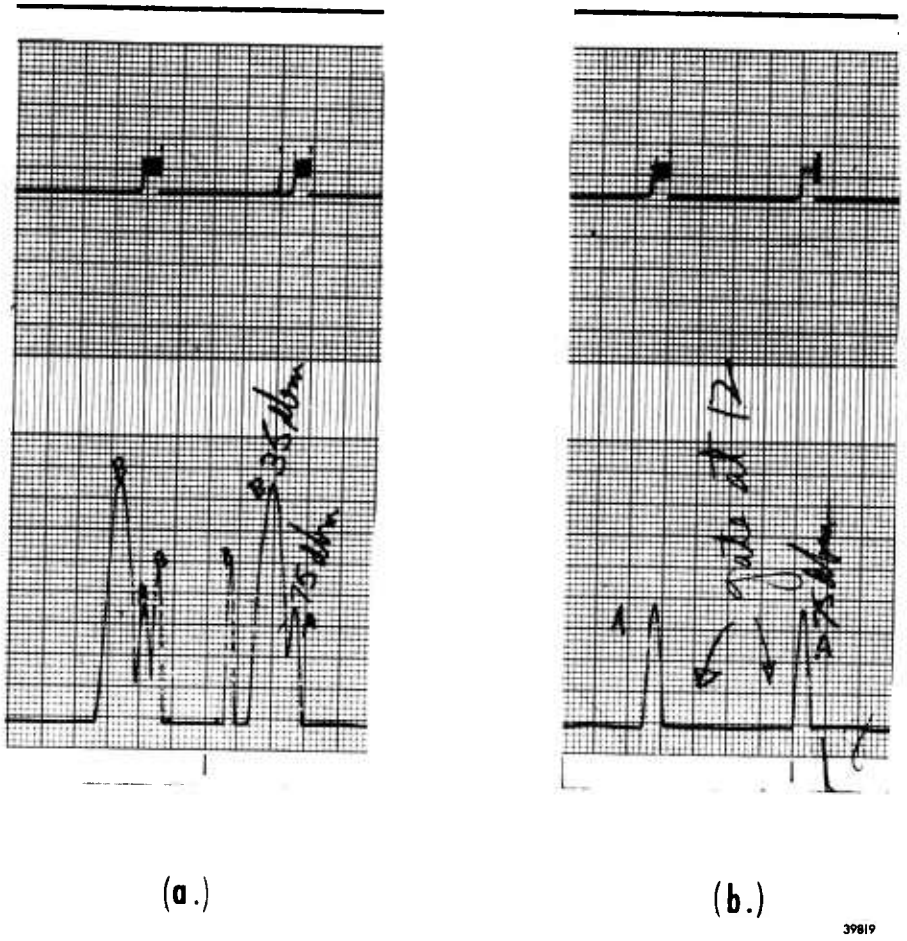

Figure 9. Oscillographs - Test III

to the Verona test site for field testing. The purpose of these tests was to demonstrate that the chosen design approach for a monitor system is feasible and to further demonstrate that all performance requirements set forth under Item I exhibit A of the contract could be met.

2.3.2 Test Facilities Description

All field tests were conducted from a mobile measurements van located at the Verona test site on the west corner of the intersection between the main entrance and Germany road. This location is marked on a rough map of the Verona site shown in figure 10. Radars are designated by circled numbers which correspond to a numbering system previously designated by RAUMA personnel.

A block diagram of the field test set up is shown in figure 11. The "Loop Vee" receiving antenna was located on a mast approximately 15 feet above ground level. As indicated in figure 11 there was approximately 23 feet of RG9 cable between the antenna and the input to the TWT amplifier. This length together with some allowance for fitting losses would produce approximately four db attenuation at 3 GC.

The physical location for the test van was chosen for convenience and terrain condition considerations and was not the optimum location for minimum path length differences between radars. Consequently for the purpose of the feasibility tests, the monitor threshold was adjusted to approximately -90 dbm. This threshold setting made it possible to record signal levels down to

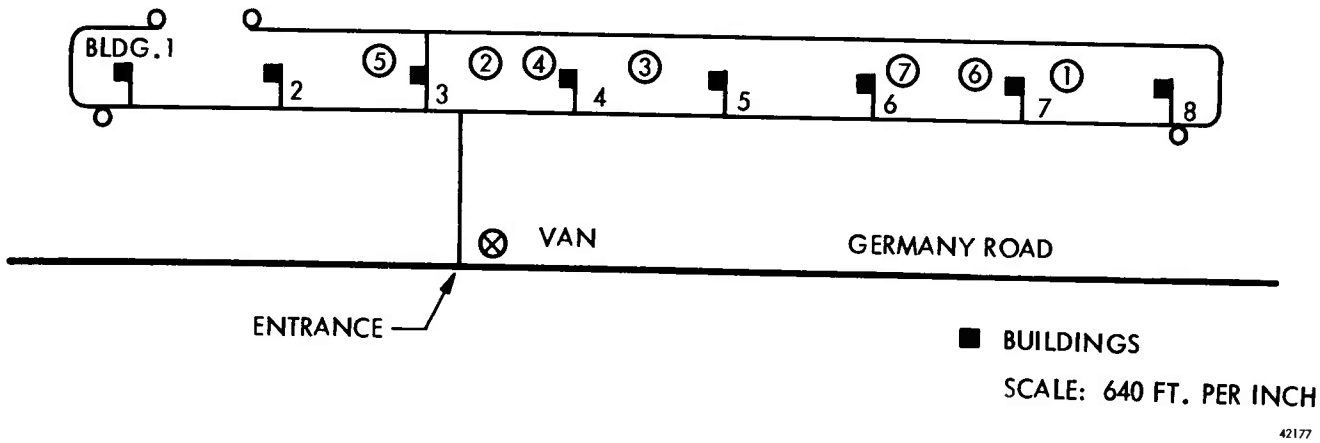

Figure 10. Verona Site, Rough Map

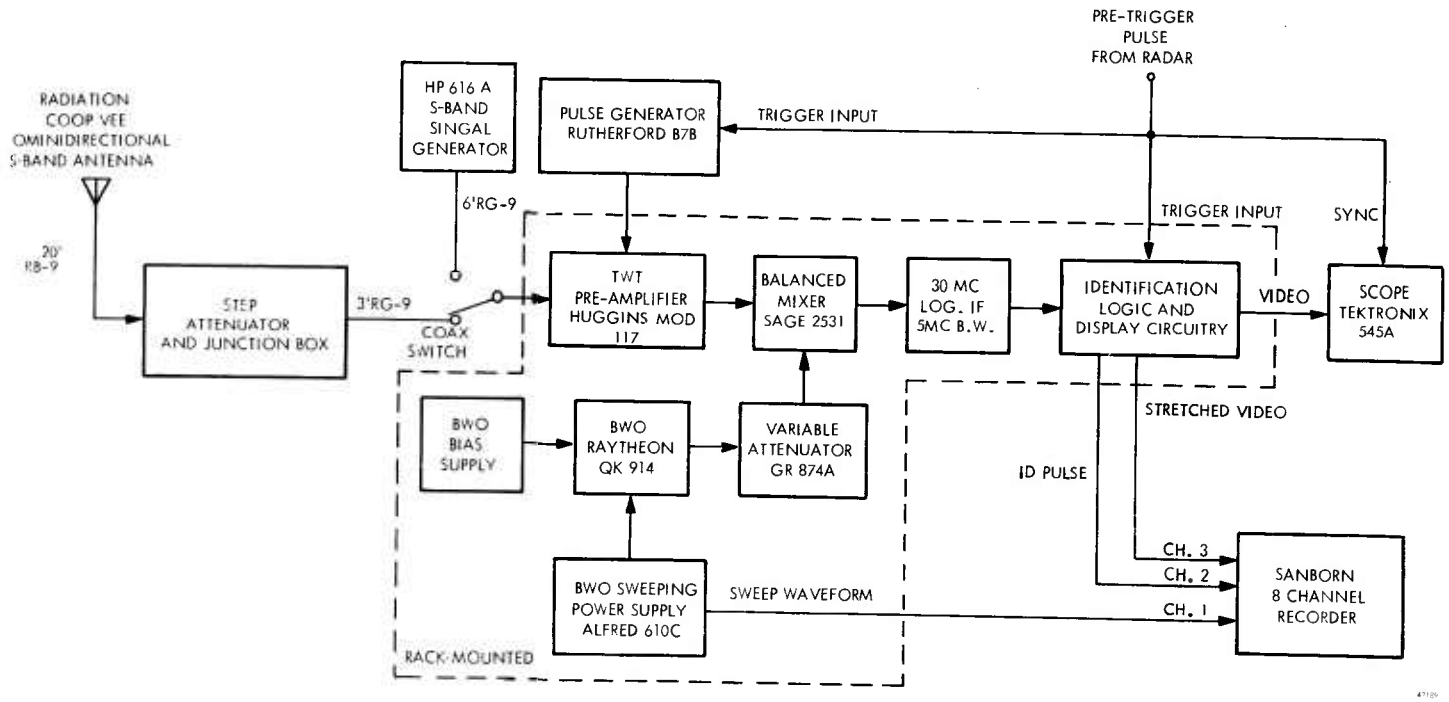

Figure 11. Block Diagram - Monitor Field Test Set Up

the monitor noise level; then by referring to a level calibration recording it was possible to determine which signals were above the level specified by MIL-R-27055 for each particular radar.

2.3.3 Preliminary Checkout and Test

2.3.3.1 General

The breadboard equipment was set up and placed into operation on Tuesday afternoon 16 April. No operational difficulties were encountered. Actual checkout and preliminary testing began on Wednesday morning 17 April. The tests made on Wednesday were mainly for the purpose of checking out equipment operation to determine if there were any problem areas such as insufficient delay between pre-trigger pulses and the arrival of the main bang RF pulse.

2.3.3.2 Calibration

After approximately 30 minutes warm up, level calibration recordings were made at four different frequencies; 2500 mc, 3000 mc, 3500 mc and 4000 mc. The recordings were made using the HP 616 S band signal generator as a signal source with a pulse width of 6 micro-seconds and a PRF of 360 cycles per second. A calibrated 6 foot length of RG 9 cable was used between the signal generator and the TWT input, and this cable loss was compensated for in setting the signal generator output level. The actual calibration recordings are

reproduced in figures 12 and 13. The numbers at each level indicate db below one milliwatt reference level. The IF amplifier compression is quite evident in these recordings. To properly interpret the meaning of the calibration level recordings in connection with measuring the signal level of an actual analog signal recording, at least two main factors must be considered:

(a) The antenna gain and cable loss between the antenna and the TWT input must be taken into consideration.

(b) It must be realized that the peak level of recorded signal may or may not represent the maximum possible level of received signal at that particular frequency when the radar antenna beam width, PRF, antenna slew rate, and monitor sweep time are taken into consideration.

Due to BWO power supply limitations, feasibility breadboard tests were run with a maximum sweep time of 100 seconds. This time is on the order of one tenth the required sweep time to guarantee a high probability of receiving the peak effective signal level from a particular radar transmitter at a given frequency during one sweep through the frequency. The effects of short sweep time are illustrated in some test which will subsequently be discussed.

For all practical purposes, the gain of the "Loop Vee" antenna can be considered to be zero db, and as mentioned previously, the average cable loss between the antenna and the TWT input was approximately four db; thus the actual level of a received signal is four db higher than indicated by the

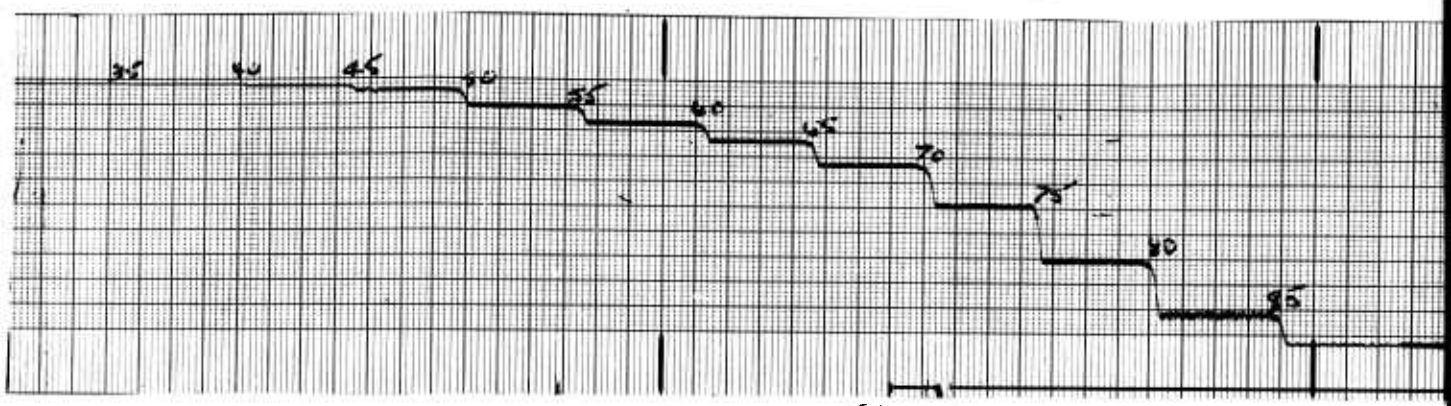

(b.) freq = 3000 Mc

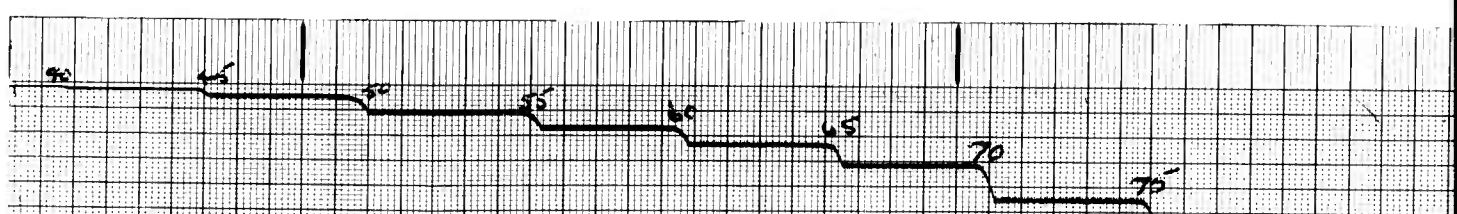

(a.) freq. = 2500 Mc

Figure 12. Oscillographs - Calibration

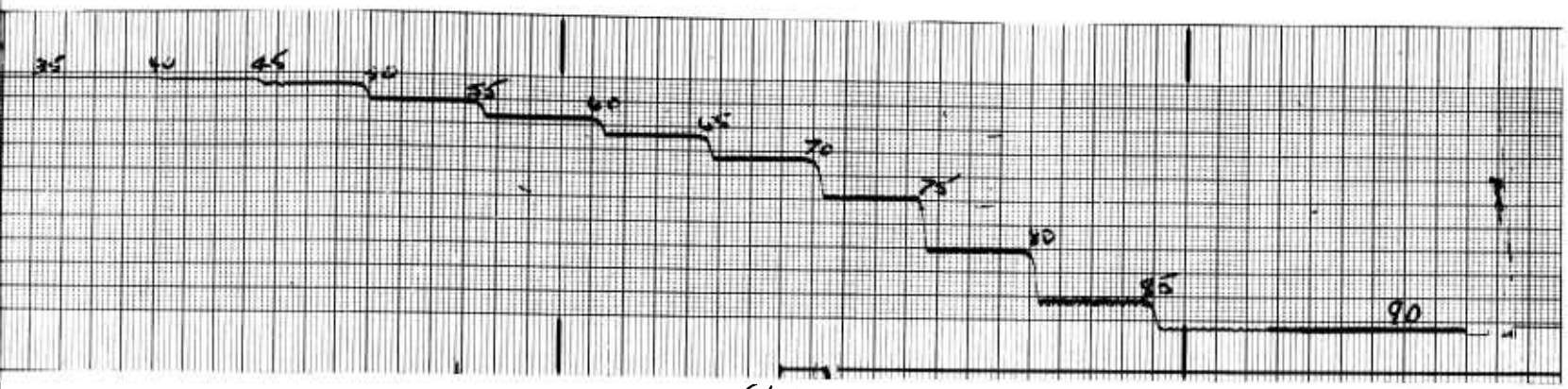

(b.) freq = 3000 Mc

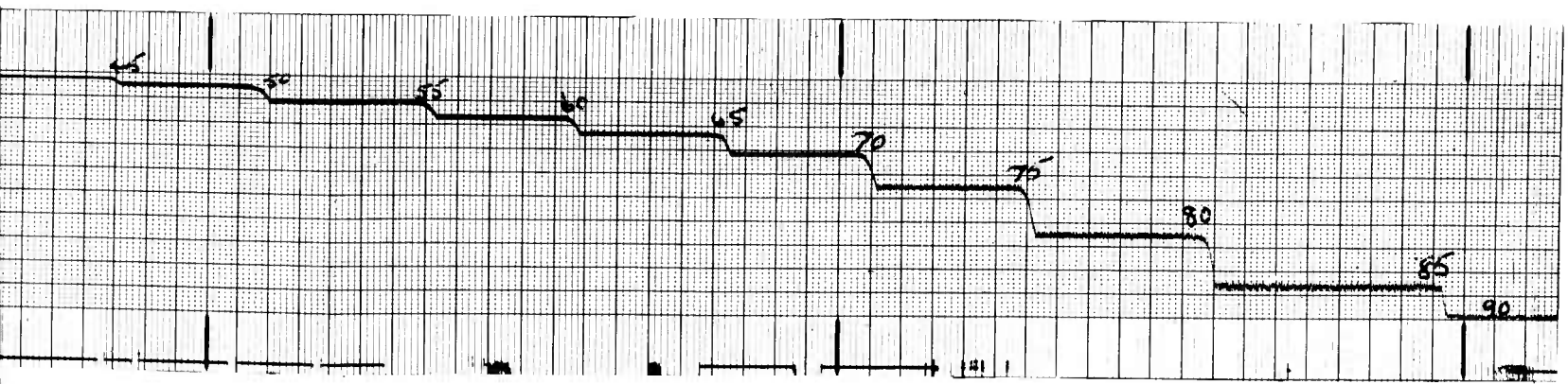

42347

(a.) freq. = 2500 Mc

Figure 12. Oscillographs - Calibration, 2.5 GC to 3.0 GC

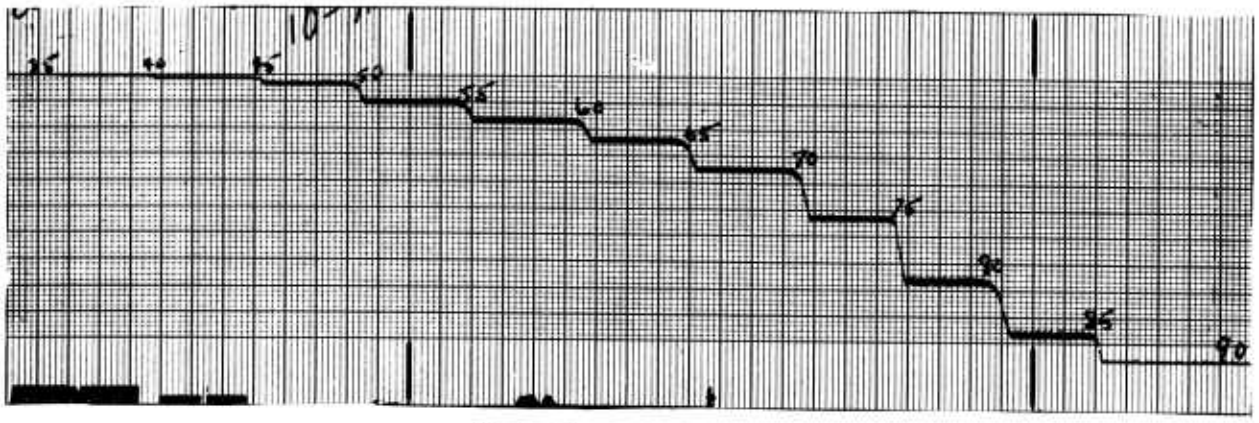

(b.) freq = 4000 Mc

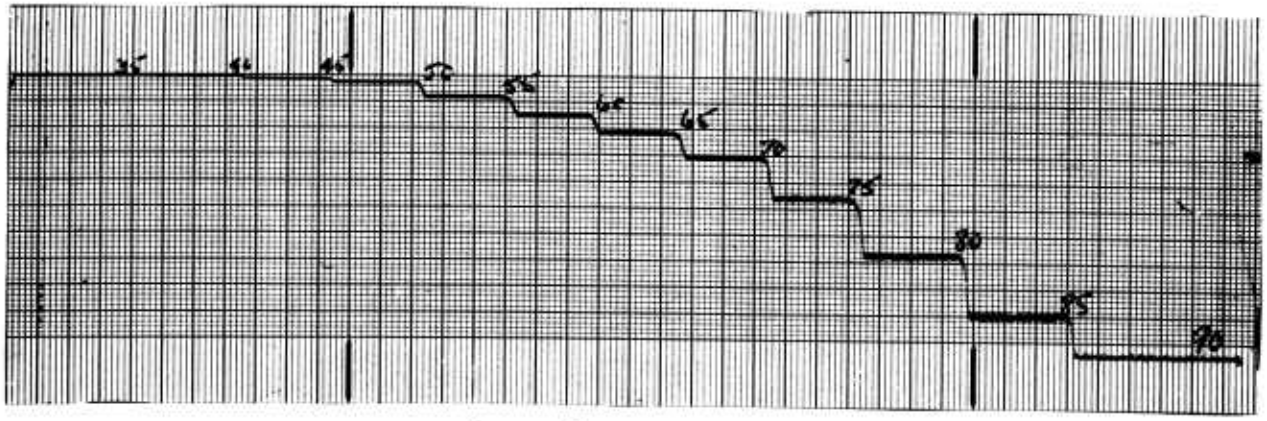

(a.) freq = 3500 Mc

42348

Figure 13. Oscillographs - Calibration, 3.5 GC to 4.0 GC

recorded level. In order to determine whether a particular received signal exceeds the specification level as defined by MIL-R-27055, it is only necessary to compare the corrected recorded level with the level computed from the following equation:

$$P_r \text{ dbm} - 20 \text{ Log } (12.1d)$$

where d is the distance in feet from the monitor site to the particular radar.

2.3.3.3 Signal Reception and Identification Checkout

For a preliminary checkout on an actual radar a pre-trigger pulse from Radar 4 was brought out to the measurements van. Radar 4 was operating at a fundamental frequency of approximately 1270 mc., a 6 microsecond pulse width of 360 pulses per second, and slewing at approximately six rpm. All other radars were supposed to be turned off. The recorded output of the monitor is reproduced in figure 14a. Channel one is the identification channel, hereafter referred to as the I.D. channel. Identification is indicated by a positive deflection from channel center of approximately 7.5 millimeters. Channel two is the detected video output. Frequency coverage (2300-4000 mc) and time extend from right to left. As discussed previously, the recorded video signals show both the signal and image separated by twice the IF frequency or 60 mc. An examination of figure 14a indicates four large signals present. Two of these signals are shown by the I.D. channel to be signals from Radar 4.

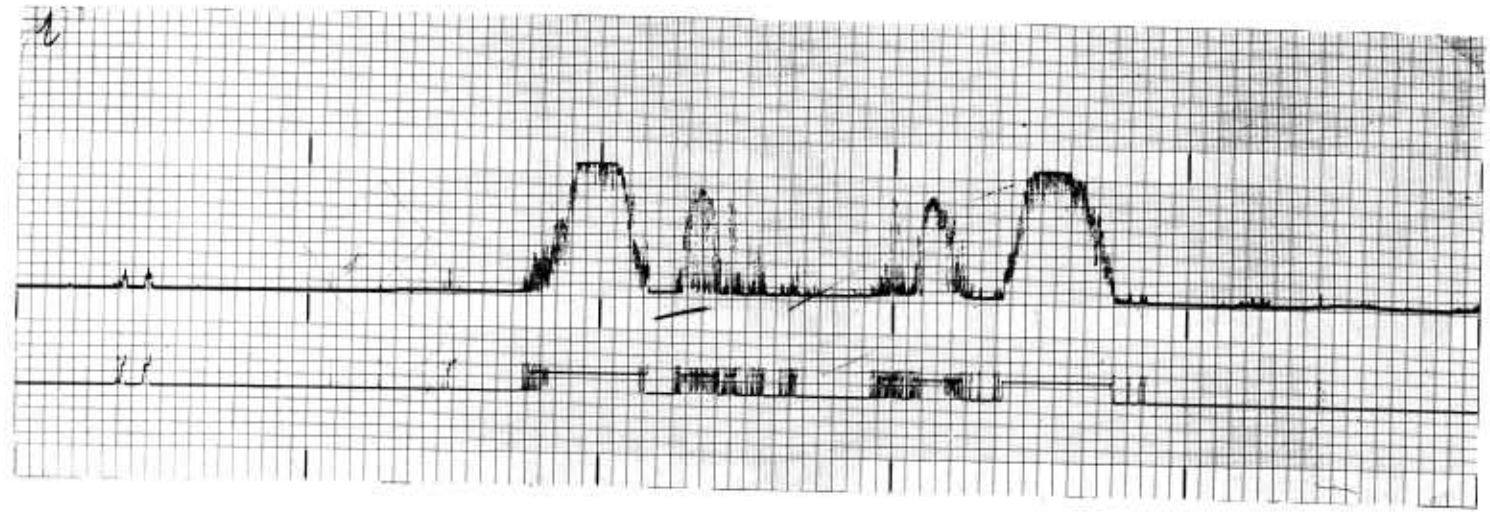

B.

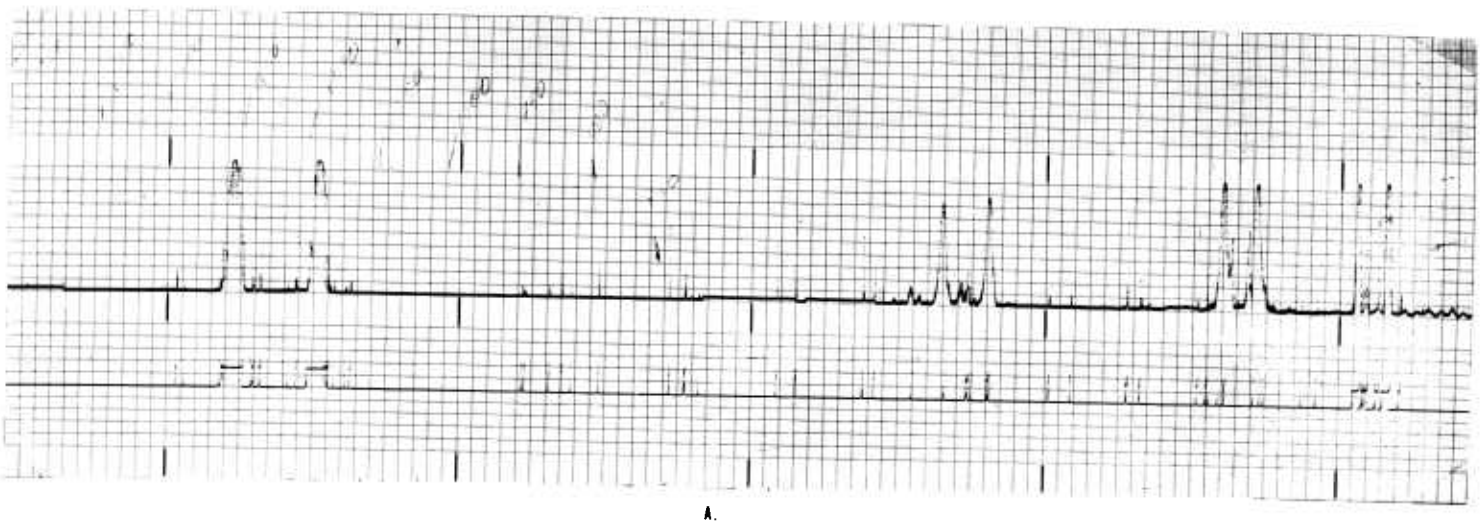

A.

Figure 14. Oscillographs - Preliminary Test I

By noting BWO tuning voltages and comparing with the BWO calibration curve, figure 20, these two signals can be identified as the second and third harmonics of Radar 4. The other two signals are not identified and therefore are not transmitted from Radar 4. The frequencies of the unidentified signals were determined and a check of the test site revealed another radar operating. The radar will hereafter be designated as Radar X. Radar X was not slewing and its operating characteristics are similar to Radar number 2. Due to the nature of the particular tests being conducted with Radar X, this radar was not turned off except momentarily in order to positively identify it as the source of the signal at approximately 2800 mc. The other signal at approximately 3140 mc was not positively identified as Radar X at this time; however, in a later test when Radar X was turned off both signals disappeared.

The reproduced recording in figure 14b was run in order to take a more detailed look at a received signal, in this case the second harmonic of Radar number 4. The sweep time was 100 seconds with a total frequency dispersion of approximately 200 mc. Chart speed was 5 millimeters per second. Since real time was from right to left and the BWO frequency swept from a lower frequency on the right to a higher frequency on the left; then the first large signal on the right occurred at the time when the frequency of the received signal minus the frequency of the BWO was 30 mc. The second large signal occurred when the frequency of the BWO minus the frequency of the received signal was 30 mc. The two lower level signals in between were produced when the frequency

difference between signal and BWO or vice versa was 15 mc. The 15 mc signals travel through the IF because of the previously mentioned diode effects. The ultimate monitor receiver would incorporate adequate filtering between the mixer and IF amplifier so that these signals would be eliminated or attenuated below the receiver threshold. Variations in appearance between signal and image can be explained when it is realized that the radar antenna was rotating and that the observed signal was the second harmonic of the radar fundamental frequency. Rapid variations in amplitude would then be possible over a relatively small slew angle due to the lobe structure of the radar antenna second harmonic pattern. This could easily account for the rapid amplitude variations indicated on the second 15 mc difference signal.

A similar checkout was run late in the afternoon with the pre-trigger input from Radar number 3. During this checkout Radars 3 and 4 were the only transmitters operating. Radar 3 was operating with a 1.3 microsecond pulse width and a 875 cycle PRF. A second run was made with the antenna of Radar 3 rotating at approximately 20 rpm. These two recordings are reproduced in figure 14. As indicated by the I.D. channel there was an almost constant signal from Radar 3 over the entire frequency band. The average level was on the order of -70 dbm. The fundamental frequency of Radar 3 was at an indicated 725 volts on the BWO sweep or approximately 3360 mc. The period between signal level nulls shown in figure 15b corresponds to the time for one antenna revolution of Radar 3.

B.

A.

Figure 15. Oscillographs - Preliminary Test 2

2.3.3.4 TWT Gating Checkout

Referring to the block diagram figure 11, the pre-trigger pulse from Radar 4 was used to trigger a Rutherford B7B pulse generator whose output was adjusted to be time coherent with the arrival of the main bang RF pulse from Radar 4. The output of the B7B pulse generator was used to gate off the TWT preamplifier time coincident with the arrival of the RF pulse from Radar number 4. Due to the multiple reflections at the particular measurement site location, it was necessary to adjust the B7B for a gate width of approximately 25 microseconds. A negative pulse of approximately 20 volts amplitude was required to reduce the level of the second and third harmonics of Radar 4 below the monitor threshold. After the gate was properly adjusted, a 100 second 2300-4000 mc recording was made with the gate off. Radar 4 and Radar X were operating. In order to make frequency identification more precise, the BWO sweep wave form was also recorded. The low frequency end of the sawtooth (right end of recording) represents +250 volts on the BWO helix and the high frequency end (left end of recording) represents +1325 volts on the BWO helix. During approximately the same time period, a recording of the same frequency range was made on the Stoddard NM62A. The NM62A recording is reproduced in figure 16, and the monitor recording is reproduced in figure 17a. Immediately after the monitor recording was run, a second 100 second recording was run. All conditions were the same as the first recording except that Radar number 4 was gated off. This recording is reproduced in figure 17b. Due to a smaller dynamic range and higher threshold of the Stoddard NM62A, the

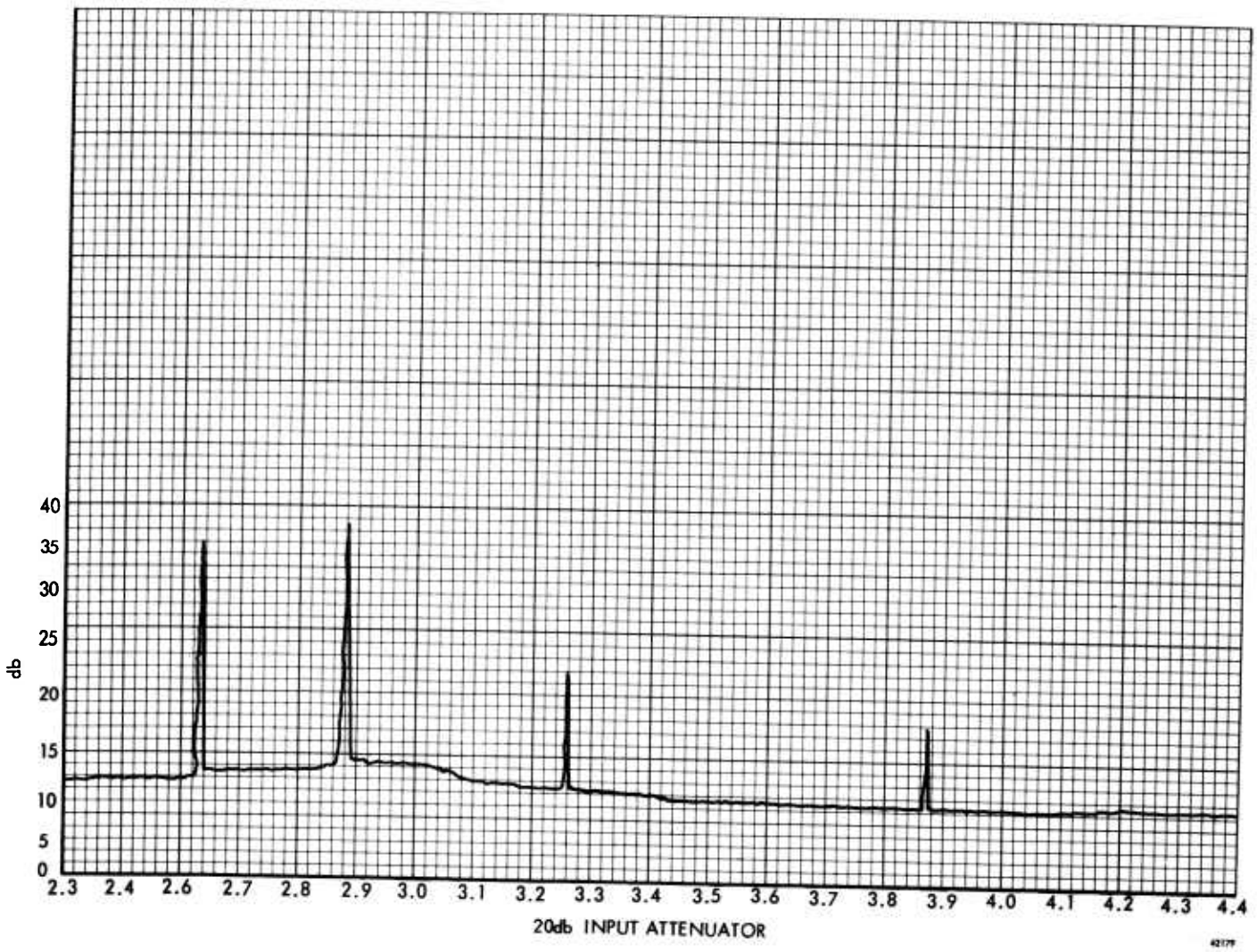

Figure 16. X-Y Plot - NM62A

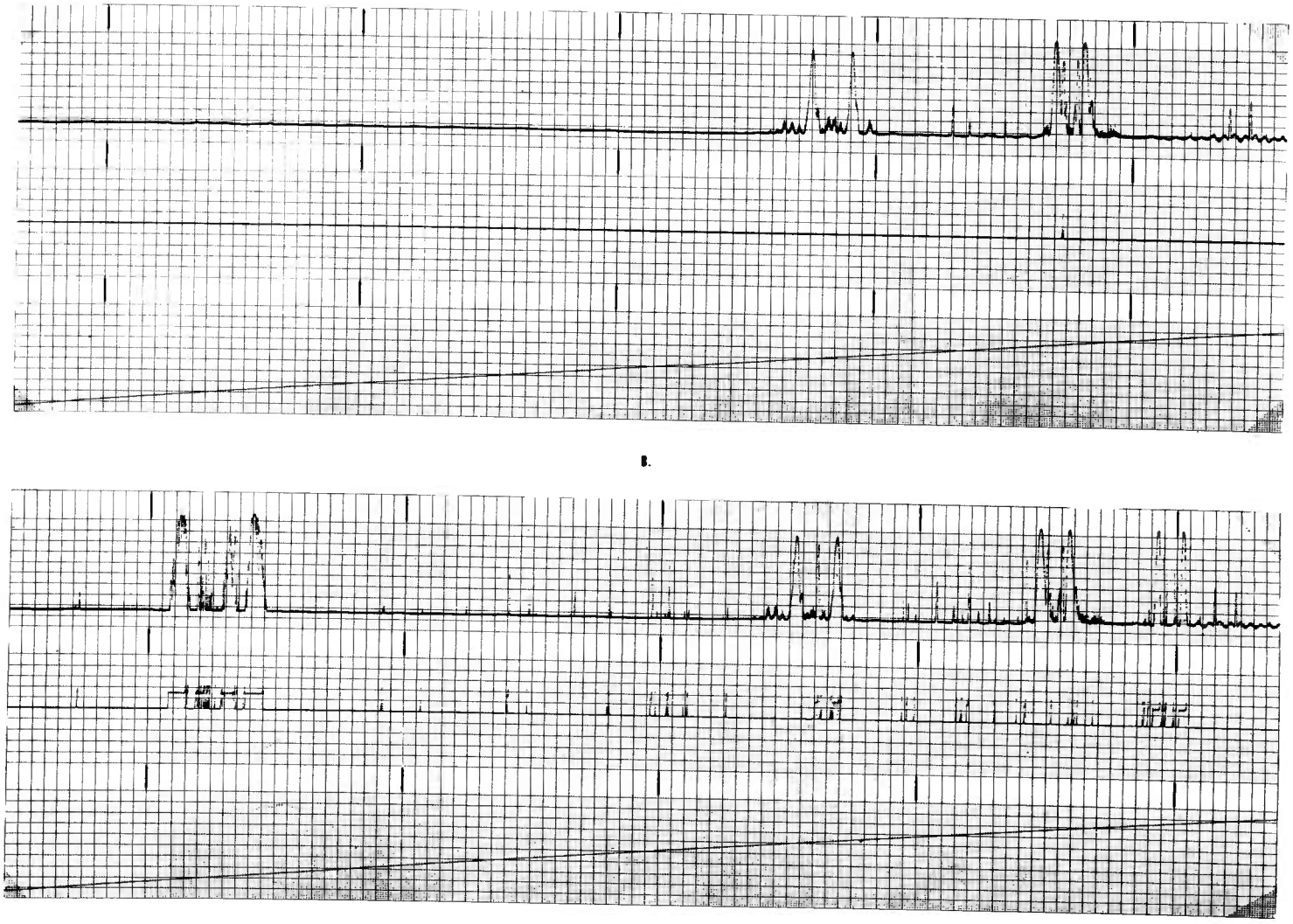

B.

A.

Figure 17. Oscillographs - Preliminary Test 3

recording reproduced in figure 16 does not show the lower level signals. It does, however, provide good correlation between the indicated frequencies of the four largest signals shown in figure 17a. As would be expected, the recording of figure 17a is very similar to that of figure 14a. A comparison will show, however, that there are considerable differences in the fine details. These differences may be attributed to the antenna rotation of Radar 4 and the short sweep time of the monitor, thus reducing the probability of intercept on fine details. Some differences were also probably due to the three hour time difference between recordings. The recording reproduced in figure 17b illustrates the effectiveness of the TWT gating system. The very rapid recovery of the TWT makes it possible to completely gate out Radar 4 with very negligible effect on the signals from Radar X. It should be noted that a large number of low level spurious signals identified as Radar 4 in figure 17a which could have been assumed to be false identifications are actually shown by figure 17b to be valid signals since they disappear when Radar 4 is gated off. On Thursday morning, April 18, several recordings were made to check out TWT gating with Radar 3. Various gate widths were used to observe the effects of insufficient gate width to gate out reflected signals. These recordings are reproduced in figure 18. Radar X and Radar 3 were both operating. Radar 3 was slewing at 20 rpm with a pulse width and PRF of 1.3 microseconds and 875 cycles respectively. Sweep time of the monitor was 100 seconds, but frequency dispersion was reduced to approximately 250 mc. Figure 18a shows the results with no gating while figure 18b shows the

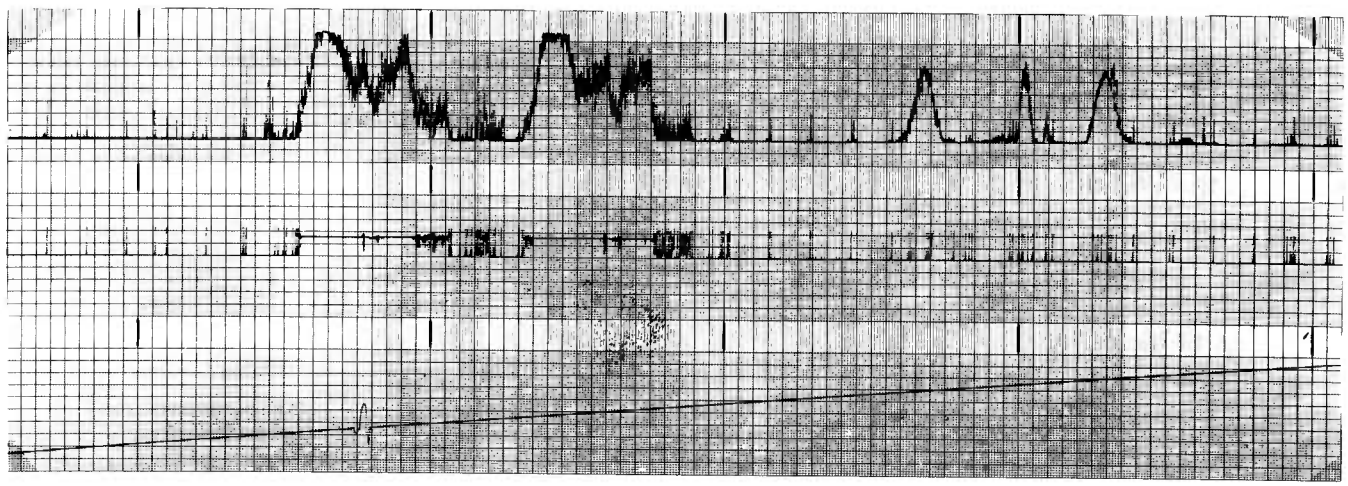

B.

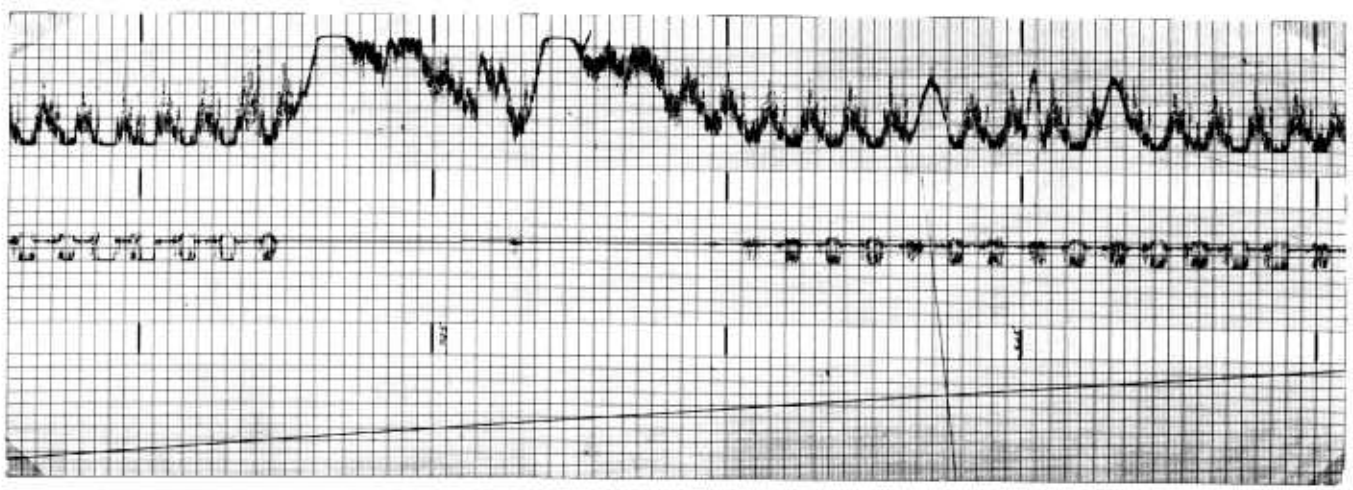

A.

Figure 18. Oscillographs - Preliminary Test 4

results with a 4.5 microsecond gate width. A 30 microsecond gate width (not shown) completely eliminated all signals from Radar 3. Since the received pulse width stretched out to approximately 25 microseconds at the fundmental frequency due to multiple reflections, the 4.5 microsecond gate affected only about one fifth of the received pulse width. At spurious frequencies the received pulse width was much narrower due to the much lower amplitude of the reflected signals. This is illustrated in figure 18b where the 4.5 microsecond gate effectively removes the spurious signals from Radar 3 but only slightly affects the amplitude of the fundamental. A discontinuity may be observed in the BWO sweep wave form shown in figure 18b. This was caused by a line transient due to air conditioner turn-on in the measurements van.

2.3.3.4.1 Partial Gating Check

The recordings reproduced in figure 19 illustrate the effects of changing the TWT gate level. The important point illustrated is that the TWT gate can be controlled in amplitude, and with proper calibration it represents a means for inserting a known gain change or attenuation which affects only the signals from a particular radar.

2.3.4 Final Testing

2.3.4.1 General

Final testing began on Thursday, April 18. The following tests discussed are designated 18-1, 18-2, etc., where 18 indicates the date and the

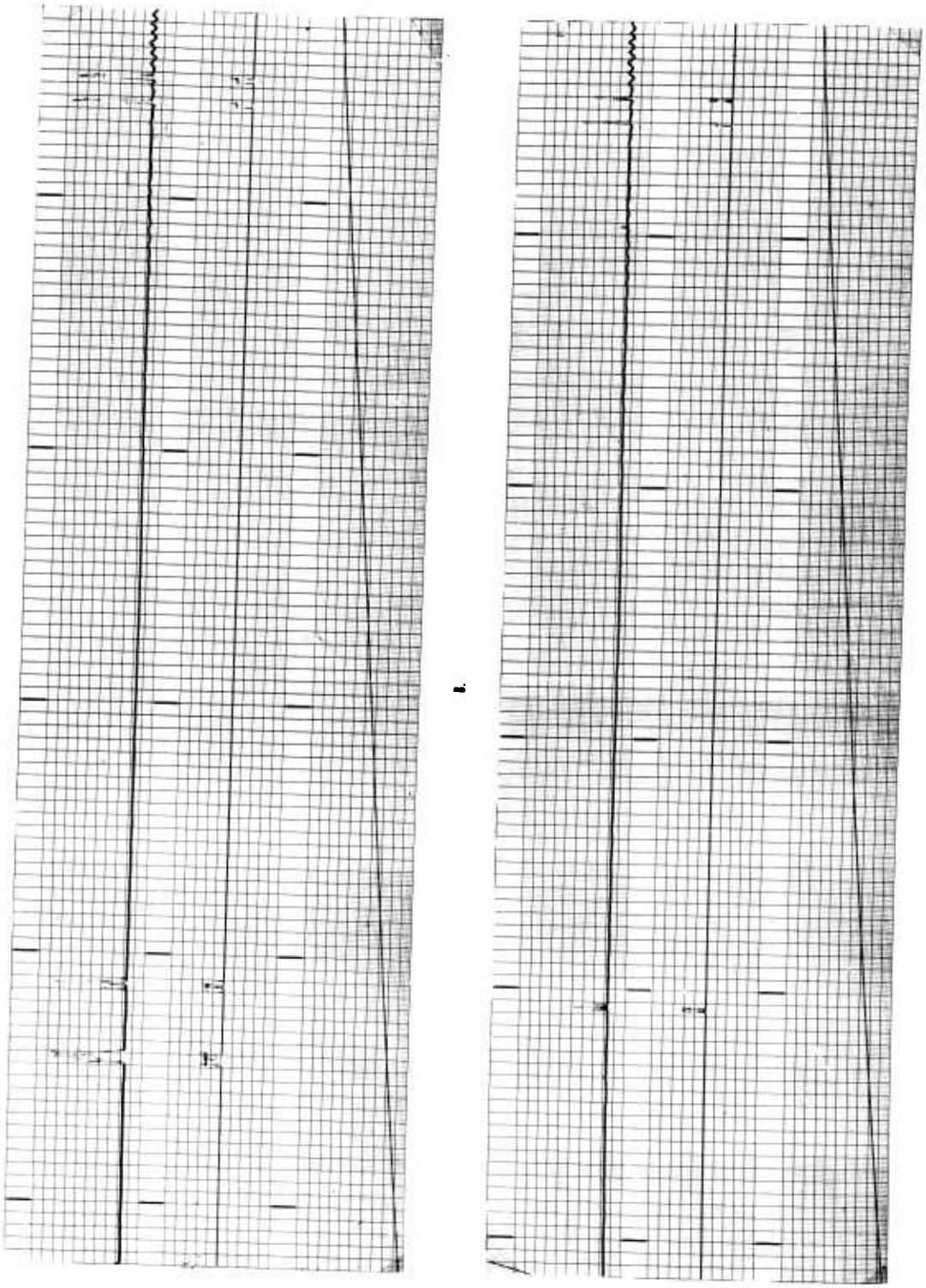

Figure 19. Oscillographs – Preliminary Test 5

dash number indicates the sequence.

2.3.4.2 Test 18-1

2.3.4.2.1 Test Objective

(a) To demonstrate the identification of a particular radar signal in the presence of others.

(b) To demonstrate the effect of gating out the signal being identified as a check on the identification system.

2.3.4.2.2 Test Conditions

Radars Operating: 3, 4 and X

Radar Operating Characteristics

Radar	Pulse Width	PRF	Slew Rate	Fundamental Frequency
3	1.3 usec	875	20 rpm	3360 mc
4	6 usec	360	5 rpm	1270 mc
X			Stationary	2800 mc

Monitor Operating Characteristics

Sweep time - 100 seconds

Chart speed - 5 millimeters per second

Frequency dispersion - 2399 mc - 4000 mc

TWT gate - 30 microseconds on Radar 3

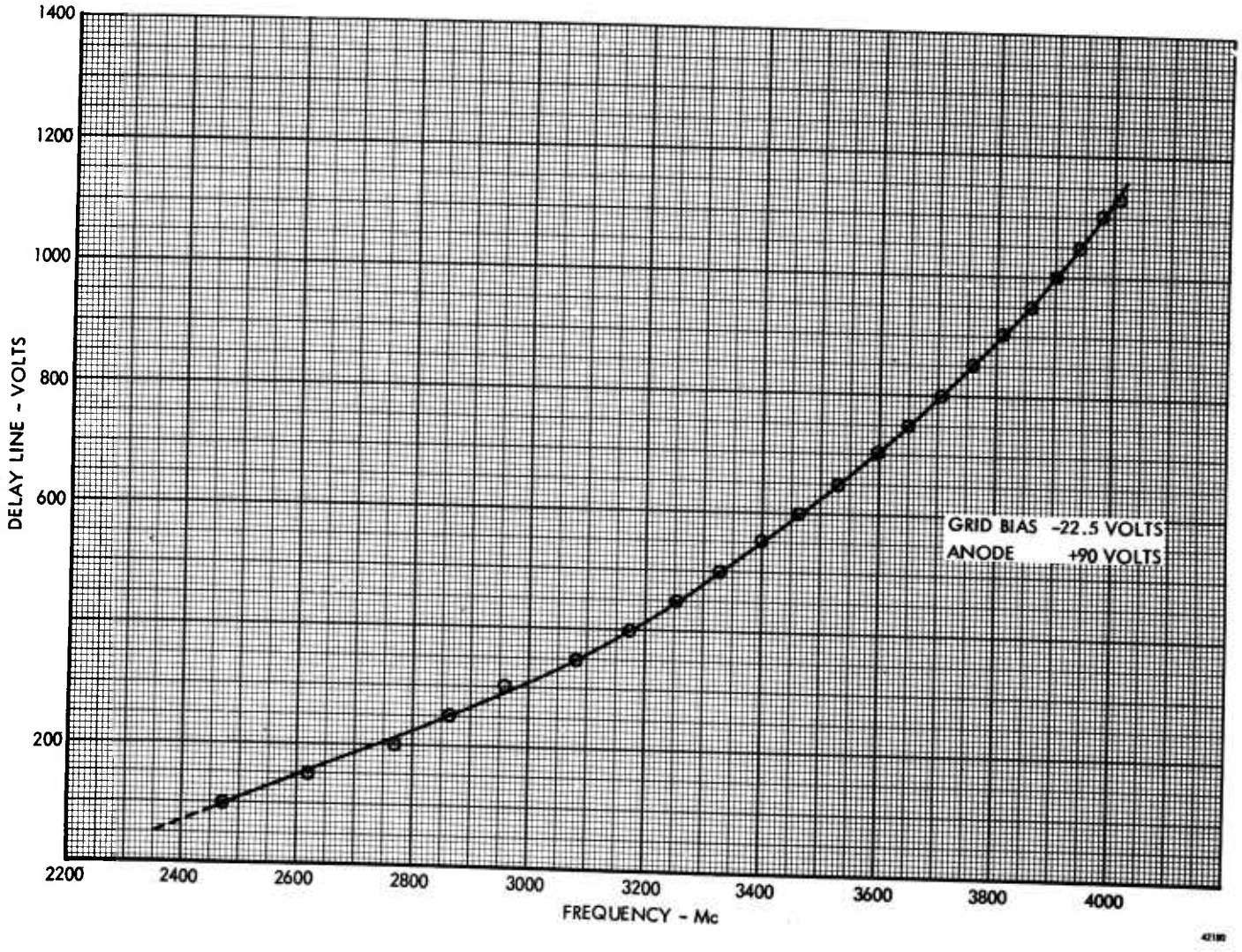

Figure 20. Curve BWO, Frequency vs Volts

2.3.4.2.3 Test Results

The recorded results for this test are reproduced in figure 21. As indicated by the I.D. channel in figure 21 there was an almost constant signal from Radar 3 over the entire frequency band. The average peak level was on the order of -70 dbm. The fundamental frequency of Radar 3 falls at about 725 volts on the BWO sweep waveform. The period between nulls in the signal level corresponds to the time for one antenna revolution of Radar 3. The second and third harmonics of Radar 4 are visible at approximately 325 and 1120 volts respectively. Also visible are the fundamental and a spurious signal found to be from Radar X at 420 and 625 volts respectively. Figure 21b was recorded under the same conditions as figure 21a except that Radar 3 was gated out. It can be seen from 21b that the removal of Radar 3 also removes the pulses of identification except for a very few false indications. It is evident then that the identification indicated in figure 21a is valid. The identification system is particularly well demonstrated in the vicinity of the third harmonic of Radar 4 where a solid identification of Radar 3 is indicated. It can be seen in figure 21B when Radar 3 is gated out that this identification is no longer present and that, in fact, a strong signal from Radar 3 was present at the same frequency as the third harmonic of Radar 4.

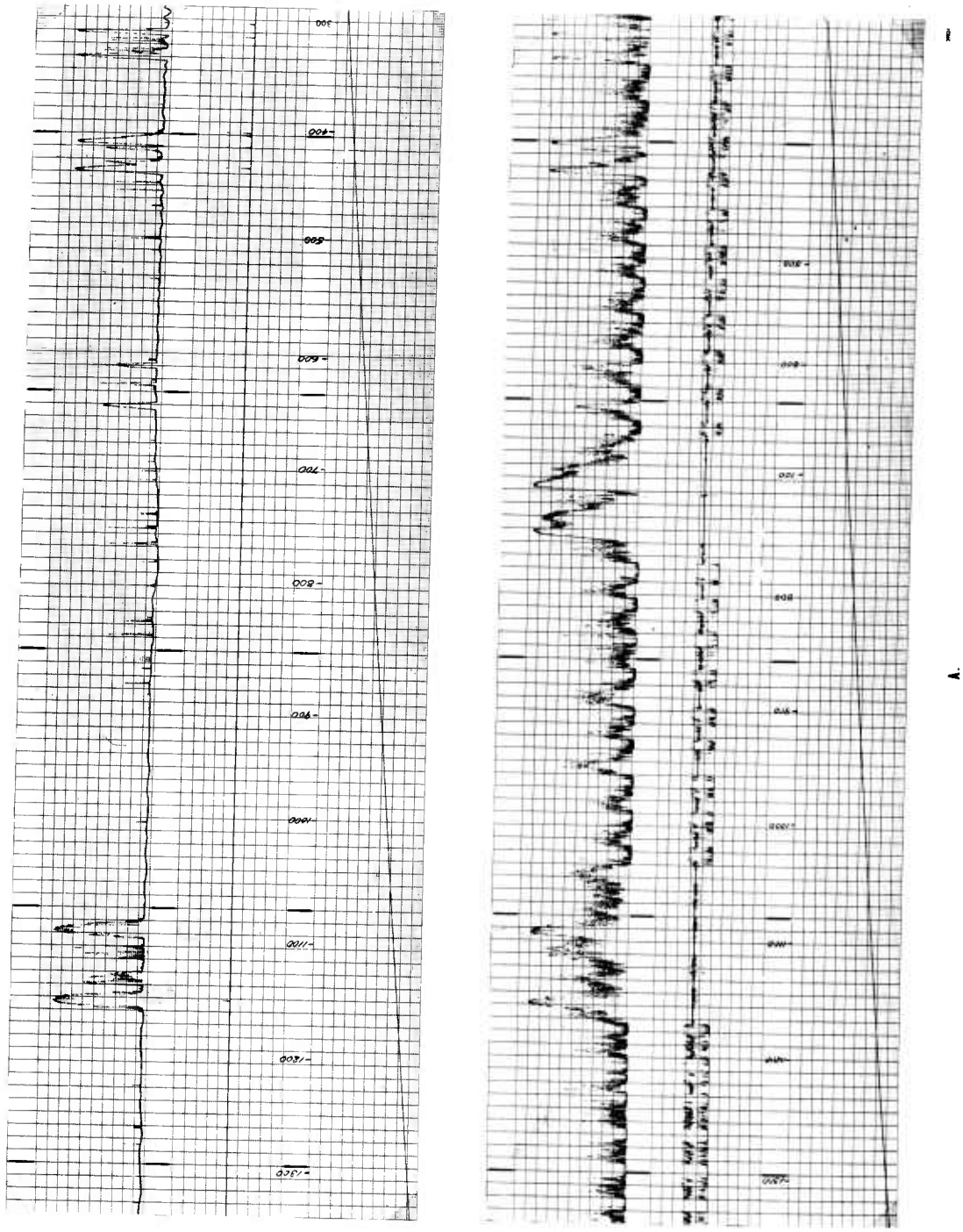

Figure 21. Oscillographs - Test 18-1

2.3.4.3 Test 18-2

2.3.4.3.1 Test Objective

To compare recorded results with recorded output of Stoddard NM62A with only Radar 3 and Radar X operating.

2.3.4.3.2 Test Conditions

Radars Operating - Radar 3 and Radar X

Radar Operating Characteristics - same as test 18-1

2.3.4.3.3 Test Results

The spurious spectrum of Radar 3, as recorded by the breadboard monitor, appears in figure 22a. A recording proceeding concurrently using a Stoddard NM62A appears in Figure 22b. The corresponding waveforms of interest are labeled A, B, C, D and E on each recording. Results the correlate appear in the following table:

	Amplitude (dbm)		Frequencies (kmc)	
Waveform	Breadboard	Stoddard	Breadboard	Stoddard
A	-50	-53	2.82	2.82
B	-65	-68	3.22	3.20
C	Sat.	Sat.	3.38	3.38

Two prominent waveforms, D and E, appearing on the Stoddard recording do not appear prominently on the breadboard recording. Note, however,

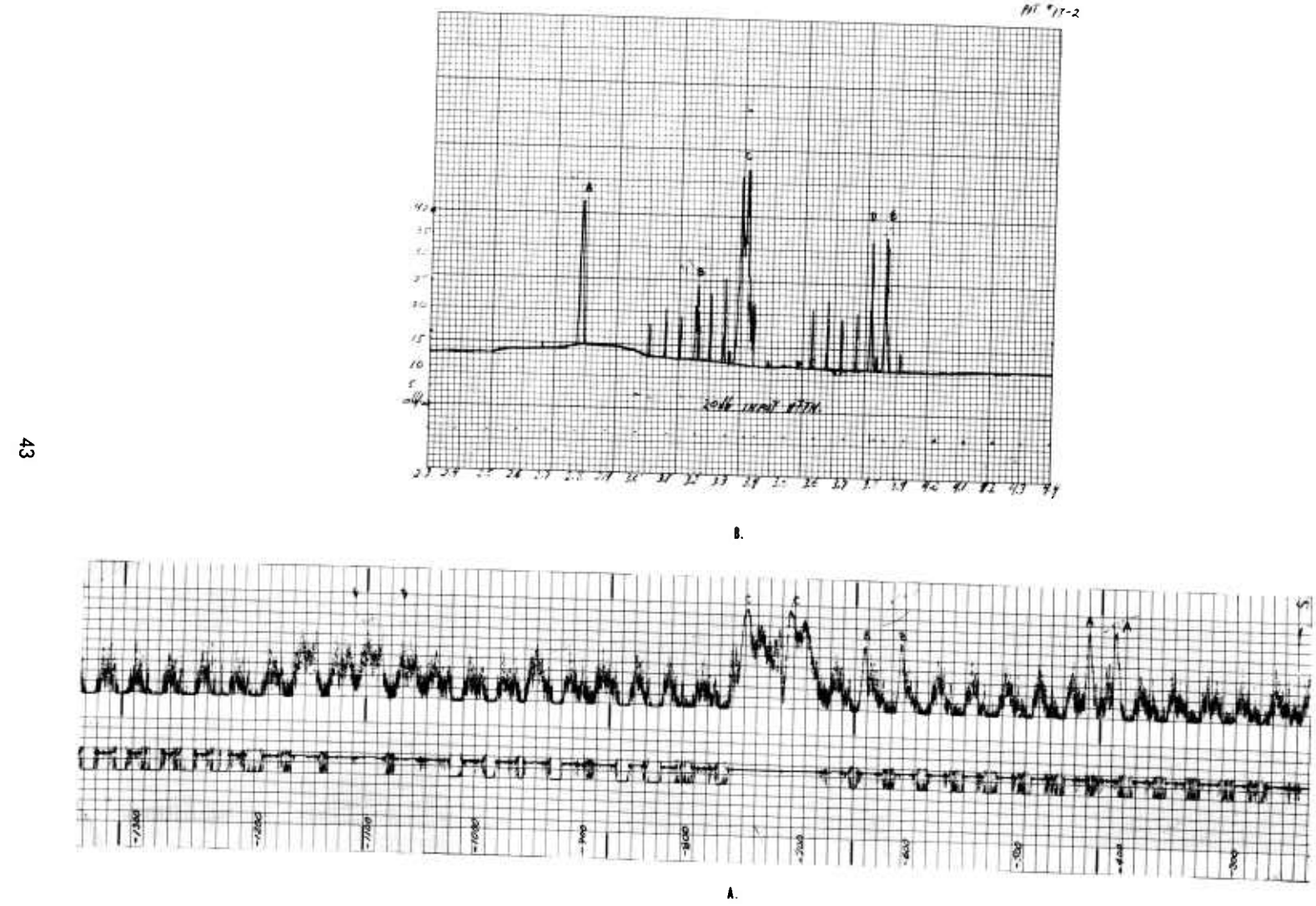

Figure 22. Oscillographs - Test 18-2

that although no numerical correlation is evident, a general increase in the spurious activity manifests itself in the vicinity (frequency-wise) of the D and E waveforms on the breadboard recording.

2.3.4.4 Test 18-3

The objective of this test was to record the spectrum of a number of radars operating with fundamental frequencies in a number of bands.

2.3.4.4.1 Test Conditions

Operating Radar	Band
2	S
3	S
4	L
5	L
6	L
7	Low UHF
X	S

2.3.4.4.2 Test Results

The recorded results of this test appear in Figure 23. Note how the entire frequency range is covered with spurious emissions. Radar 3 accounts for a large portion of the interference as found previously. This test indicates the

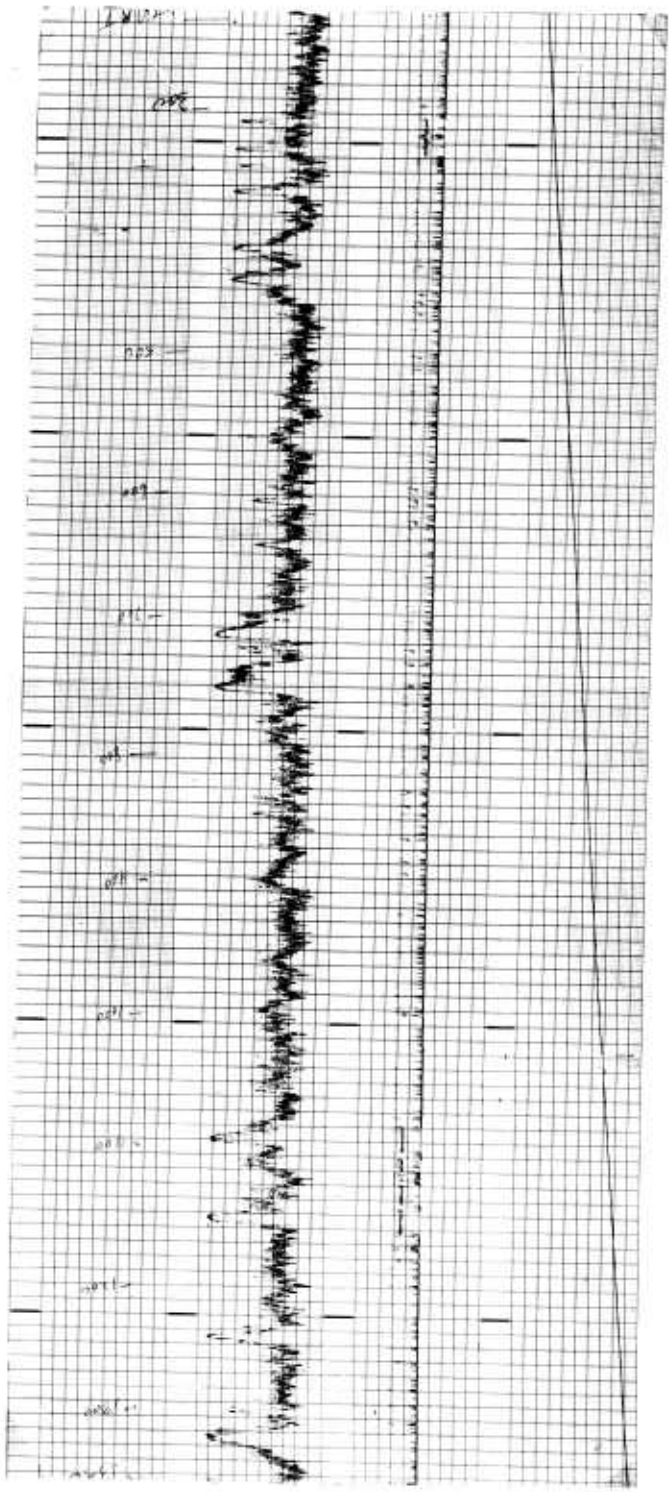

Figure 23. Oscillographs - Test 18-3

dire need for TWT blanking gates to prevent known RFI offenders from obscuring the recording of spurious signals from other radars.

2.3.4.5 Test 18-4

The objective of this test was to record the interference spectrum in S band of a radar having a low fundamental frequency.

2.3.4.5.1 Test Conditions

Radar 7, having a low fundamental frequency was operating. All other Radars except Radar X were turned off.

2.3.4.5.2 Test Results

A recording of results appears in Figure 24. The unlabelled waveforms are caused by Radar X as determined in previous tests. It is thought that waveforms A and B are caused by Radar 7 because they appear to be harmonically related to its fundamental. A complete identification system would have verified this one way or the other.

2.3.4.6 Test 18-5

The objective of this test was to demonstrate identification and TWT blanking.

2.3.4.6.1 Test Conditions

Radars 4 and 5 and X are operating. Identification and blanking is associated with Radar 4.

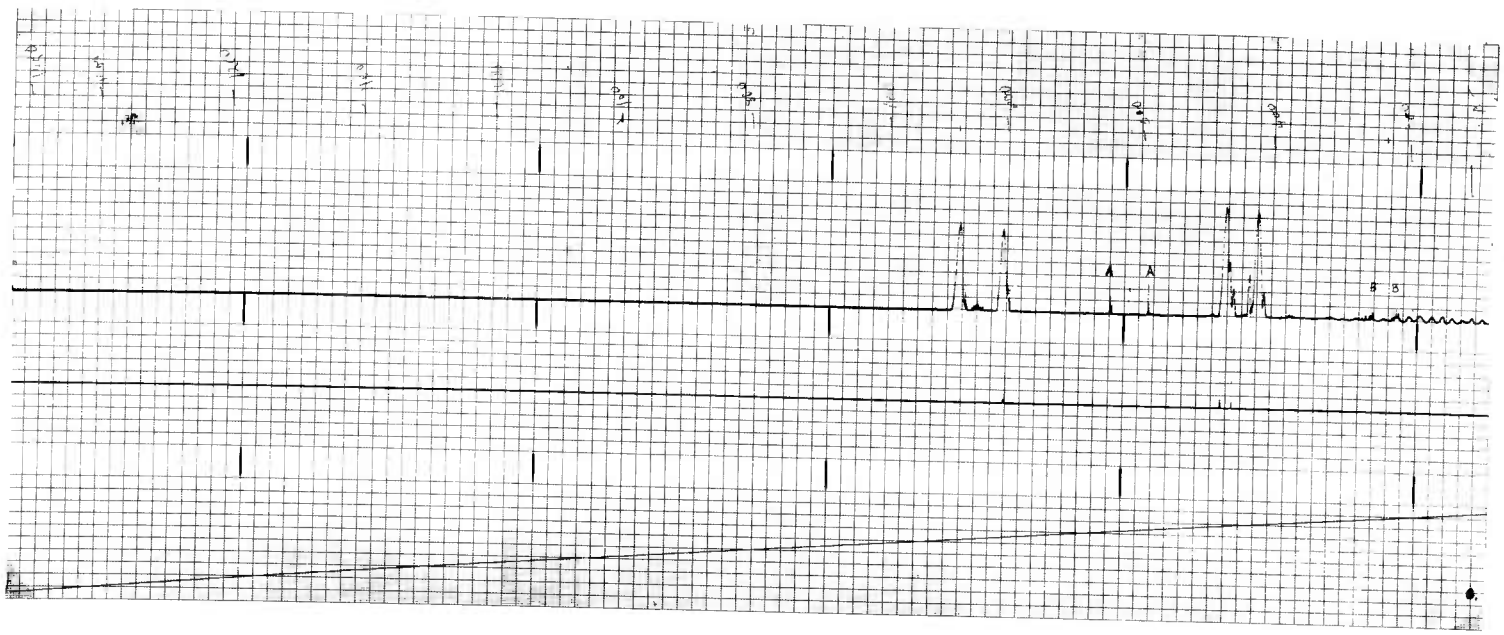

Figure 24. Oscillographs - Test 18-4

2.3.4.6.2 Test Results

The recorded results appear in figures 25a and 25b. Figure 25a shows the results with no TWT blanking and figure 25b shows the results with Radar 4 blanked out. Note in figure 25a that radar 4 is identified throughout the spectrum by I.D. pulses. In figure 25b, both the interference and identification of Radar 4 are missing as a result of blanking.

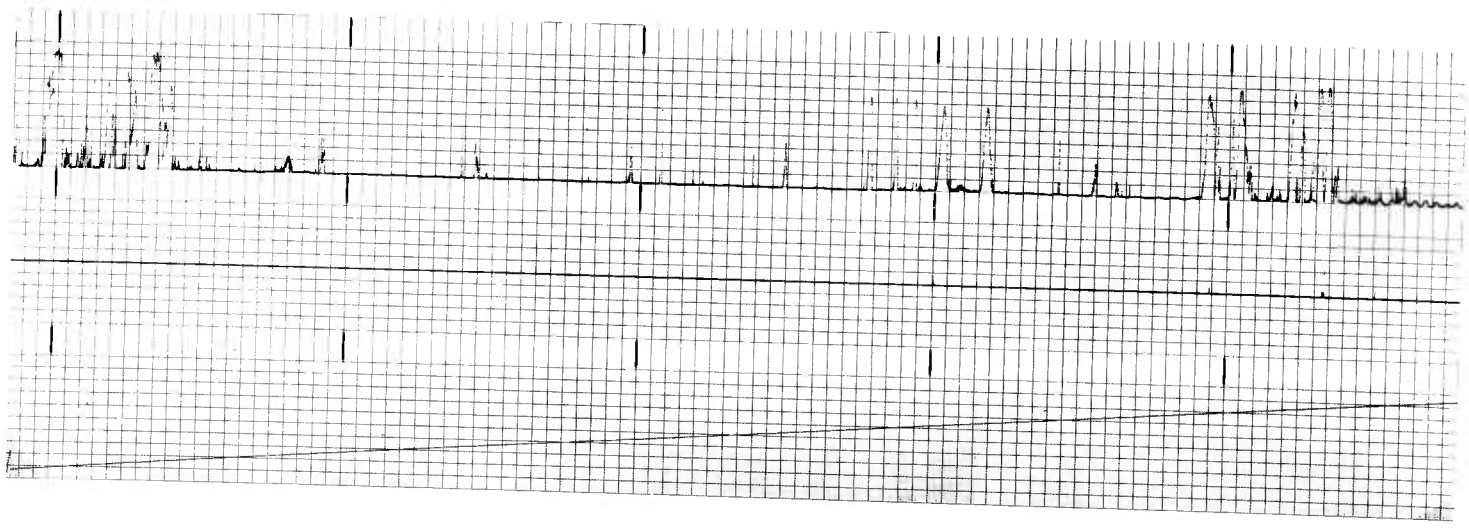

B.

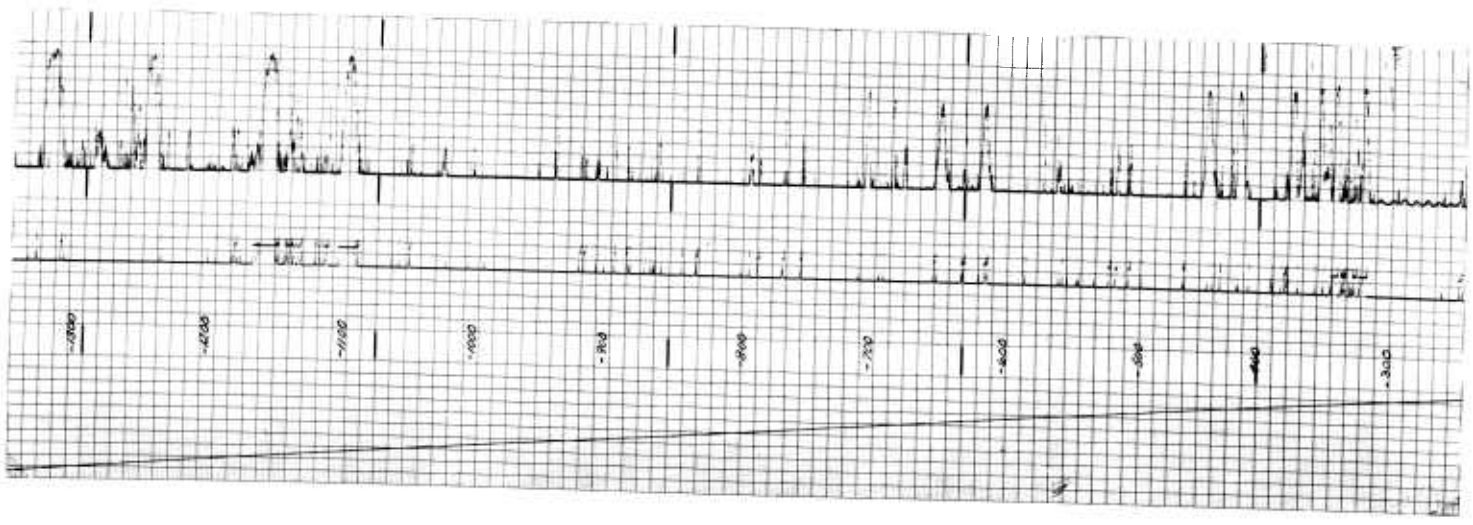

A.

Figure 25. Oscillographs – Test 18-5

3.0 ULTIMATE MONITOR

3.1 Modification to Original Approach

3.1.1 Identification Logic

The occurrence of false identification in both the laboratory and field test results indicates the need to modify the original identification approach slightly. False identification occurs because of a random process in which the "on time" of two or more radars occurs simultaneously. To review the identification process, reference is made to the simplified block diagram of Figure 26. When properly aligned, the delayed pretrigger pulse R1 is time coincident with the R1 pulse derived from the main bang RF of Radar 1. Fulfillment of the coincidence requirement results in the triggering on the recorder. Suppose, however, that the RF sub-system is tuned to another Radar frequency, that of Radar 2. As long as the Radar 2 RF pulse is not time coincident with the Radar 1 RF pulse (the majority situation) then the B1 pulse derived from Radar 2 is not time coincident with the R1 pulse and no false triggering of the I.D. one-shot occurs. If the two RF pulses are coincident, however, false identification results. The probability of false identification with the present design is a function of the pulse repetition rates of Radars 1 and 2, the B1 and R1 pulse widths, and the length of time the monitor receiver stays tuned to Radar 2 (the number of B1 pulses derived from Radar 2 during the sweep).

An attempt has been made to derive the general equation expressing the probability of getting one false identification during one receiver

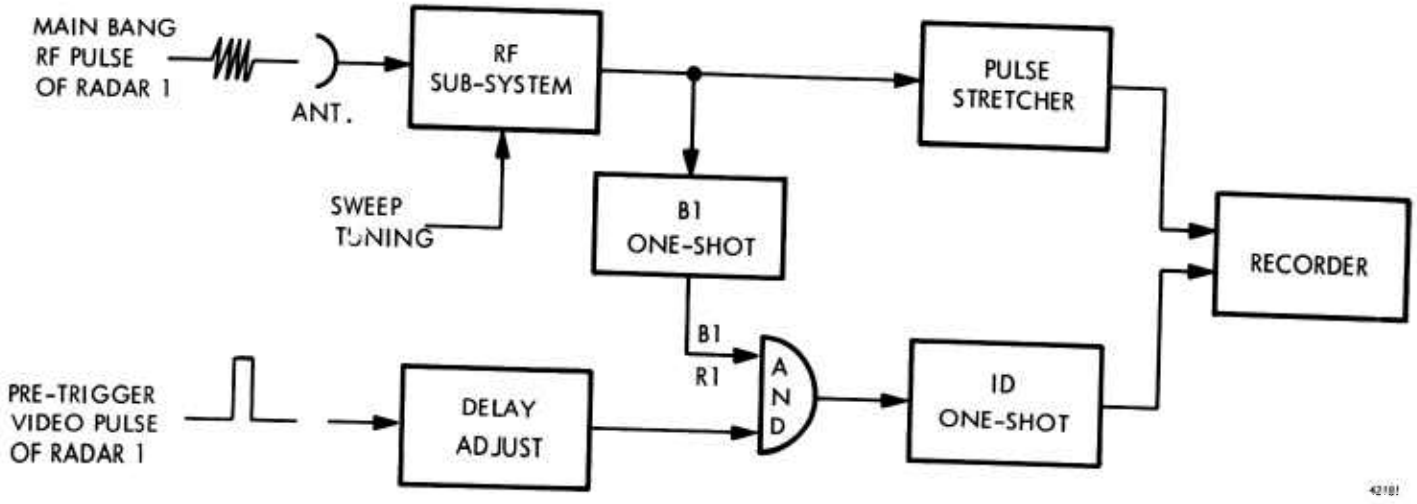

Figure 26. Block Diagram - Breadboard Monitor

sweep through the frequency of Radar 2. It became apparent, however, that the expression so derived is useless in a practical case. For example, suppose that the repetition rate of Radar 2 is exactly 2000 pps and the repetition rate of Radar 1 is exactly 20 pps. Since one is an exact multiple of the other (implying synchronism) their "on time" is either always coincident or never coincident dependent upon the phase relationship between them. For non-synchronous signals one needs to know what error is involved in assigning repetition rates to the signals. Assuming the 2000 pps to be exact, the probability of coincidence during a given time interval is then a function of whether the second repetition rate is really 20 pps or 20.01 pps or 20.001 pps and so on. Since this degree of accuracy in specifying repetition rates is not normally known, the usefulness of a generalized probability of coincidence is severe enough to present a number of false identifications in both the laboratory and field test results.

A solution may be realized by prescribing that a certain number of consecutive coincidences be required before identification is made. If the two repetition rates are vastly different, the chance of getting two coincidences in a row is extremely remote. The worst case occurs when the two repetition rates are very close together and they happen to be "crossing each other" (as viewed on a scope). The number of consecutive coincidences occurring during the crossover is a function of the repetition rates and pulse widths as expressed in the following equation:

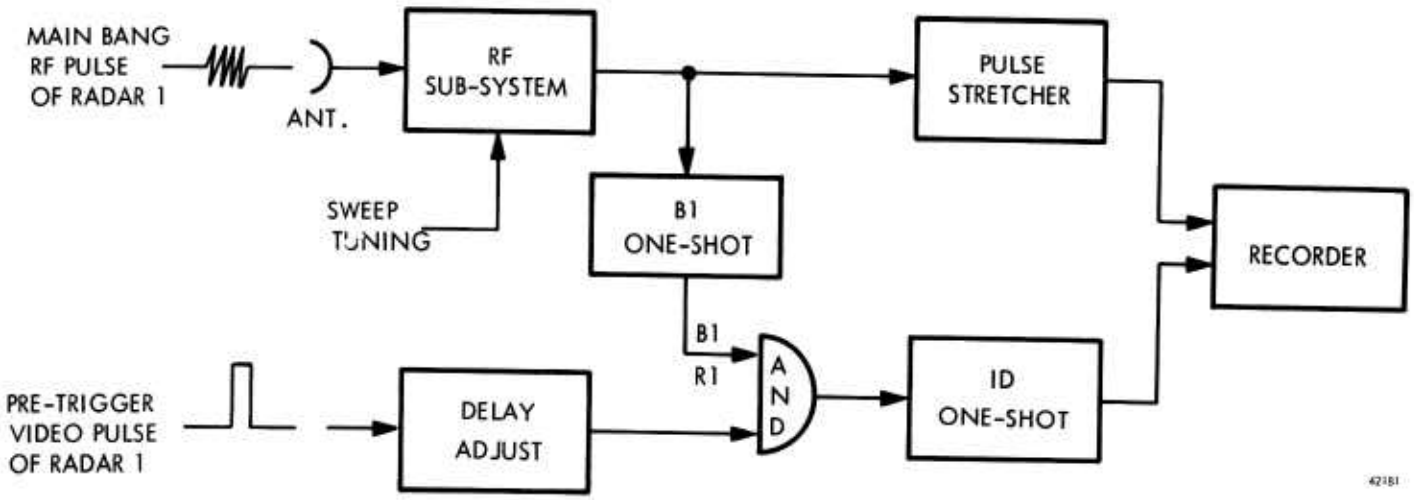

Figure 26. Block Diagram - Breadboard Monitor

sweep through the frequency of Radar 2. It became apparent, however, that the expression so derived is useless in a practical case. For example, suppose that the repetition rate of Radar 2 is exactly 2000 pps and the repetition rate of Radar 1 is exactly 20 pps. Since one is an exact multiple of the other (implying synchronism) their "on time" is either always coincident or never coincident dependent upon the phase relationship between them. For non-synchronous signals one needs to know what error is involved in assigning repetition rates to the signals. Assuming the 2000 pps to be exact, the probability of coincidence during a given time interval is then a function of whether the second repetition rate is really 20 pps or 20.01 pps or 20.001 pps and so on. Since this degree of accuracy in specifying repetition rates is not normally known, the usefulness of a generalized probability of coincidence is severe enough to present a number of false identifications in both the laboratory and field test results.

A solution may be realized by prescribing that a certain number of consecutive coincidences be required before identification is made. If the two repetition rates are vastly different, the chance of getting two coincidences in a row is extremely remote. The worst case occurs when the two repetition rates are very close together and they happen to be "crossing each other" (as viewed on a scope). The number of consecutive coincidences occurring during the crossover is a function of the repetition rates and pulse widths as expressed in the following equation:

$$(1)^* \quad \Delta N = \frac{(t_1 + t_2)\, f^2}{f}$$

where

N = Number of cansecutive caincidences

t_1 = pulse width af Radar 1

t_2 = pulse width of Radar 2

f = nominal repetition rate af either

Δf = actual difference in the repetition rates

In order for this equation to be useful, an educated guess must be made as ta how close the repetition rates are likely ta be in determining Δf. Obviausly, for synchranized signals, Δf is zera and N is infinite (the derivatian assumes phase caherence). This unique case is of na particular concern, however, since synchronized received signals are nat anticipated under actual field conditions due to path length differences. For non-synchronous signals twa types af repetitian rate generation may be considered: (1) two signals having repetition rates derived from crystal controlled oscillatars of the same frequency (non-adjustable) and (2) two signals having the same nominal repetition rates derived from tunable oscillators. The first case is by far the hardest to handle since the repetition rates are stabilized to the point where pulse coincidence could last indefinitely. Perhaps the best approach in this special case is simply to live with the problem; the recorder notes that the interference generated is fram either of two saurces. For further definition, one of the radars is turned off and the test is re-run over the frequency spectrum of interest. The second

* derived in appendix

case may be analyzed on the basis of equation (1). For a "bad case" analysis assume the following conditions:

f = 1800 pps (nominal)

$t_1 = t_2$ = 1 micro-sec. (set in monitor)

Δf 1.8 cps (-.1% of nominal)

Then, from equation (1),

$$N = \frac{(1 + 1)\ 10^{-6}\ (1.8)^2\ 10^6}{1.8}$$

$$= 3.6$$

Hence, for the conditions posed, the maximum number of consecutive coincidences is 3. A necessary requirement is that the nominal repetition rates be separated by at least 0.1% of the nominal value. In order to meet this requirement, detuning of one or the other of the repetition rate oscillators may be necessary, though unlikely. A solution in terms of the block diagram of figure 26 is to insert an integrator between the "and" gate and the I.D. one-shot such that four consecutive coincidences between B1 and R1 are required before sufficient voltage is built up to trigger the I.D. one-shot. This modification is shown in figure 27. As regards the ultimate monitor, an integrator would follow each of the "and" gates, 1 through 20, shown in Technical Note 2, Figure 8.

3.1.2 TWT Blanking Gate

As indicated in the laboratory and field test recordings, the TWT blanking gate provides the mechanism for preventing a strong interference signal

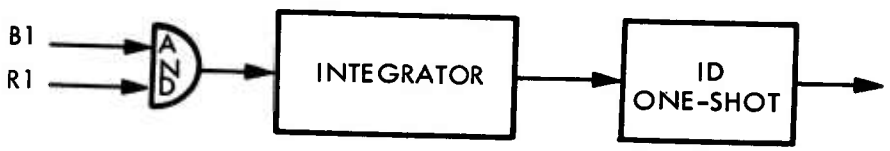

Figure 27. Modification to Eliminate False Identification

with a wide frequency spectrum from masking the results of weaker signals within the same spectrum. This is accomplished by applying to the TWT gate input terminal a gate pulse (derived from the video pre-trigger pulse) which time overlaps its associated RF pulse. The gate pulse is of such a polarity (negative) as to shut the TWT off during this interval.

It was found during field testing at Verona that the width of the blanking pulse must be appreciably greater than the transmitted pulse width in order to completely eliminate the interference data from the recorder. The reason for this became obvious when the detected RF pulse was displayed on a scope. In addition to the main bang RF pulse, there were reflections from as far away as three miles which when viewed on the scope had the apparent effect of stretching the pulse to the order of 20 times its normal width. The log characteristic accentuated this effect. The width of the blanking gate had to be increased to the point where all reflections were likewise blanked out in order to eliminate interference from this source. As regards the ultimate monitor, this means that a variable pulse width is desirable for each blanking signal, the width of which is determined in advance by terrain reflection characteristics and the transmitted power level.

3.2 Recommendations

3.2.1 Hardware Philosophy

Before defining hardware specifications for the ultimate RFI monitor, it is well to formulate a philosophy concerning the overall scope and

objectives of the monitor program. The need exists for an interference monitoring device capable of automatically recording interference data caused by a number of pulsed radar transmitters operating simultaneously. The data recorded should consist of the amplitude, the frequency, and the source identification of the interference signal. It is felt that the uncertainties introduced in amplitude measurement by site effects are sufficient to warrant considering the monitoring conceptually as an indicating device rather than an instrument of exact measurement. The usefulness of the monitor should lie in its ability to quickly scan the frequency spectrum of interest, pin-point the frequency of interference phenomena, identify the source, and give a rough estimate of the signal strength. After localizing the problem area with the monitor, more accurate amplitude information may be gathered with a number of field intensity meter measurements if desired. A chief asset of the monitor should be its ability to rapidly determine "where to look" and "at whom". In order to implement the specifications with hardware one needs to decide whether the monitor is conceptually a universal device, readily workable in any RFI environment, or a special device, designed to meet the unique requirements of a particular radar site. The nature of this decision as it relates to the implementation of the identification sub-system is particularly significant. For example, the routing of coaxial cable from each radar to the monitor for identification purposes is completely feasible at a ground radar site and completely absurd when making interference measurements on aircraft. A universal concept would dictate the need for an RF link to replace

cable connections in spite of an order of magnitude increase in cost. It is the opinion of Radiation personnel that, initially at least, the hardware design should be directed to meet the needs of the Verona test site. The reasons are as follows:

1. Verona represents a "worst case" situation where many radars may be operating simultaneously under vastly different operating conditions (power, PFR, pulse width, slew rate, etc.). Hence, a design directed to satisfying Verona's requirements tends to be universal.

2. Those features which lend universality to the device are in the nature of add-ons which can be included in future designs without major internal modifications to the basic monitor.

3.2.2 Hardware Specifications

Consideration of the above philosophy and the present availability of all major RF components permits expression of the recommended requirements of the monitor.

3.2.2.1 General

Amplitude accuracy	±10 db
Frequency accuracy	±0.5%
Identification accuracy	99%

The role of the monitor is passive. Meeting the specifications should not require an active manipulation of the transmitting equipment. Recording should be limited to those spurious signals which exceed the specification limit spelled

out in MIL-R-27055 (USAF).

3.2.2.2 Antenna Subsystem

Gain	0 db or better
Beamwidth	Adequate to cover the potential radar equipment locations
Frequency range	200 mc to 40 KMC

3.2.2.3 Receiver Subsystem

Frequency Range	200 mc to 40 KMC
Sensitivity $\frac{S}{N}$ = 10 db	90 dbm
Dynamic range	90 db minimum
Frequency resolution	±0.5%

3.2.2.4 Display Subsystem

Type storage	permanent
Information stored	1. Amplitude
	2. Frequency
	3. Identification

Positive and automatic identification of the interference source should occur simultaneously with the recording of interference signal amplitude. Identification should not be contingent upon transmitting equipment shut-down or other manipulation.

3.2.3 Hardware Implementation

It is recommended that the RFI monitor be implemented as shown in the block and logic diagram of drawing SK-504630 included in this report. Since most of the diagram has been discussed in detail sectionally in Technical Note 2, this presentation is meant as a synthesis of concepts evolved rather than a detailed discussion of any particular one.

As shown, the 200 mc - 40 KMC band is sectionalized into nine sub-band receivers each one having a heterodyned front end tuned by a common sweep generator. The antennas, although shown lumped in the same block for drawing convenience are actually sectionalized according to bandwidth before routing to the nine sub-band receivers. A block diagram of sub-band monitor #1 is shown as representative of all the other sub-band monitors. With the exception of the voltage tunable magnetron (VTM) local oscillator, the blocks are identical in each of the other monitors. After sub-band monitor #2, a backward wave oscillator (BWO) is used as the local oscillator. The traveling wave tube (TWT) acts as both an RF amplifier and an RF gate. The amplified RF signal from the TWT is mixed with the VTM local oscillator to produce a 30 mc IF signal which is amplified, detected, and amplified again before appearing at the input to the threshold network. The threshold level is established by a wave-shaping network which compensates for variations in system gain as a function of frequency. The peak difference between the signal and the threshold level is detected and stretched before being processed through a buffer

amplifier to one of the recorder channels. Frequency markers are derived from a multiple cavity having a number of resonant points at fixed frequency intervals. The detected frequency blips are used to trigger the F one-shot which standardizes the pulse width and assigns a unique pulse amplitude to the output F pulse. The third output signal from each sub-band monitor is the B pulse, derived from a one-shot which senses the time of occurrence of an interference signal at the output of the threshold network.

Video pulses R1 through R20 (to tie-down the drawing, 20 operating radars are assumed) are derived from the pre-trigger pulses transmitted along coaxial cable to the monitor from each operating radar. The R pulses are delayed in time by an adjustable "delay one-shot" until they are time coincident with their associated main bang RF pulse at the monitor. Hence the B pulse, derived as a result of interference occurring during the main bang RF pulse interval, is likewise time coincident with an associated RF pulse. Each B pulse is "anded" with every R pulse to determine coincidence and hence establish the identification of the interfering radar. To eliminate false identification, an integrator following each "and" gate requires at least four consecutive coincidences before it triggers its associated I.D. one-shot. To conserve recorder channels, four I.D. one-shots are directed to one recorder channel through an "or" gate. Identification is preserved by assigning a unique amplitude to each one-shot. Likewise, frequency markers F1 through F9 are grouped in three's and directed to one recorder channel through an "or" gate.

The TWT blanking gates, G1 through G9 are derived from the R pulses. The leading edge of each R pulse triggers a one-shot (not shown) having an adjustable pulse width. The pulse width is adjusted until it overlaps the received transmitter pulse and associated reflections. Manual toggle switches and "or" gates may be used to switch any of the derived blanking gates to any of the TWT gate inputs and, thus, inhibit selected radars from producing interference signals at the recorder. The chart recorder recommended is the Honeywell model 1508 Visicorder. The specifications are included in Technical Note 2. Seventeen of the twenty-four channels are used for data recording.

4.0 CONCLUSIONS

The work during this program was intended to define techniques which would permit the continuous monitoring of the spectrum from a number of pulse radar transmitters located near the monitoring instrument.

Since the Verona Test Site was of primary concern, initially the work included an examination and definition of the probable frequencies and levels which would be encountered from equipments in use there.

Consideration of the radar locations, expected interference properties, and the requirement for recognition of the levels defined by MIL-R-27055 (USAF) permitted the definition of the requirements of the monitor.

Approaches which would permit detection of threshold levels (MIL-R-27055 (USAF)) and positive identification of the source of the radiation were examined.

The monitor approach chosen is intended to automatically and rapidly scan the spectrum and record the approximate levels and frequencies present across the spectrum from 200 Mc to 40 Gc and indicate which transmitter on the site is causing each observed emission.

A breadboard monitor was constructed for the purpose of demonstrating the feasibility of the approach at S Band.

After laboratory tests at Radiation Incorporated, the breadboard monitor was tested in conjunction with radar transmitters at the Verona Test Site.

Although the breadboard model was equipped with only a single identification channel, the feasibility of providing positive identification of the source of received spurious powers was established. Recordings of received data demonstrate that small spurious signals are reliably recognized and identified even when obscured by higher power signals at the same frequency.

The limitations of the commercial power supply employed to sweep the Backward Wave local oscillator dictated that the slowest available sweep for the nominal octave range was approximately 100 seconds. This relatively rapid sweep is too short to provide an adequate probability of intercept under adverse conditions. Computations reported in the first Technical Note (RADC-TDR-62-505) show that a sweep time of approximately 18 minutes is required. However, even the 100 second sweep was observed to provide a reliable indication of radiated frequencies and identification of the source. This is true because the high sensitivity of the TWT monitor front end and the logarithmic receiver characteristic permit easy visual detection of small signals. Even the source of stray reflections appearing when the scanning antenna is not illuminating the monitor directly are correctly identified. Because of the fast TWT recovery time, overload of the front end from very large signals does not degrade the ability to detect and identify other signals.

The TWT preamplifier when employed with a frequency swept local oscillator in a superhetrodyne receiver provides a simple and reliable method of receiving signals of widely separated strengths. For the monitoring

of pulsed transmitter spectra no tracking tunable filters are required since the combination of frequencies, coincident time of arrival, and levels required to produce erroneous results would occur infrequently. These random errors are inhibited until three or more events are noted and hence would not appear in recordings of received data.

The availability of monitoring equipment having the characteristics realizable from the described approach would permit a ready determination of the source of spurious signals. In a dense radar environment this information could be obtained without the need for constant attendance by an operator, and without communication between the monitor site and the radars on the station.

The accumulation of permanently recorded received data and subsequent reduction by correlation with transmitting equipment logs would provide additional valuable information on the spurious signal radiating characteristics of current equipments.

APPENDIX

Equation (1) in the test is derived as follows:

With reference to Figure 28, the relative displacement, Δt, of the trailing edge of P2 relative to P1 during one pulse interval results from the fact that P1 has a slightly faster repetition rate than P2. Coincidence is maintained for the number of pulses required for the relative displacement to go through the interval t. That is;

$$N = \frac{t}{\Delta t}$$

$$= \frac{t_1 + t_2}{T_2 - T_1}$$

$$= \frac{t_1 + t_2}{\frac{1}{f_2} - \frac{1}{f_1}}$$

$$= \frac{(t_1 + t_2)(f_1 + f_2)}{f_1 - f_2}$$

$$= \frac{(t_1 + t_2) f^2}{\Delta f}$$

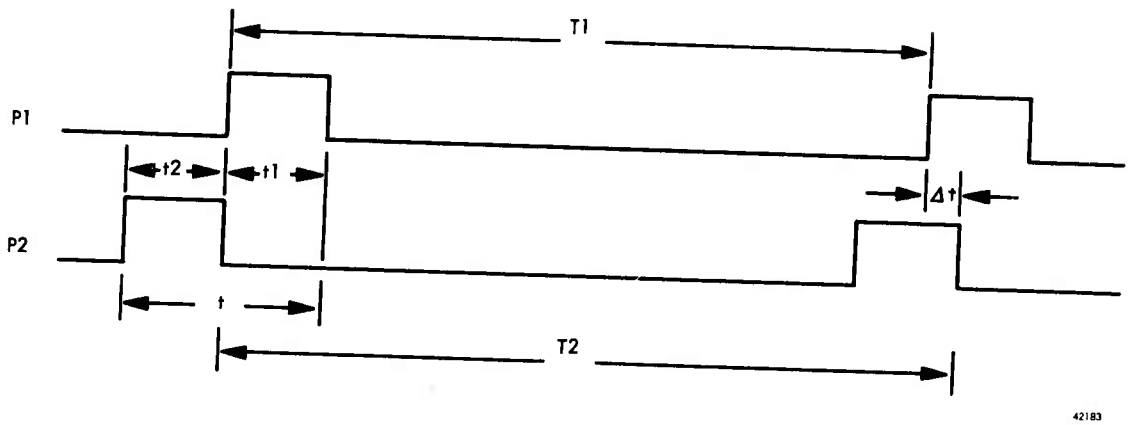

Figure 28. Relative Pulse Timing Diagram

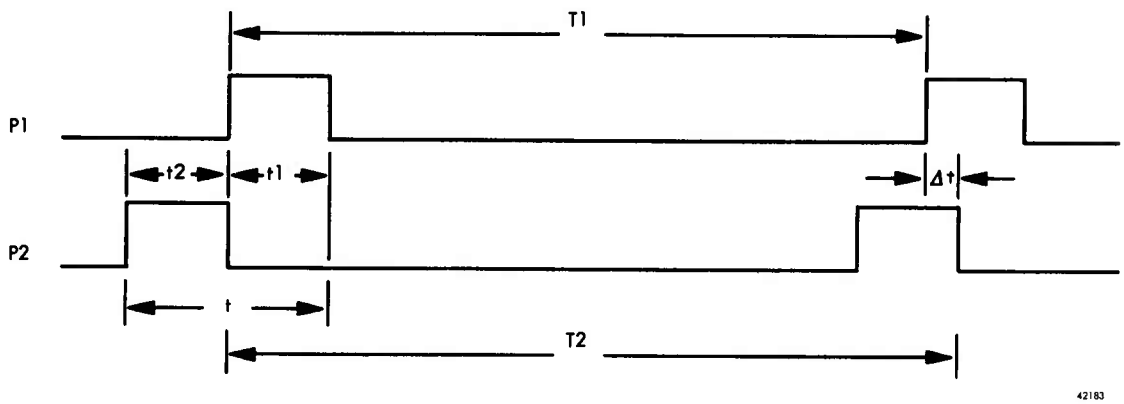

Figure 28. Relative Pulse Timing Diagram

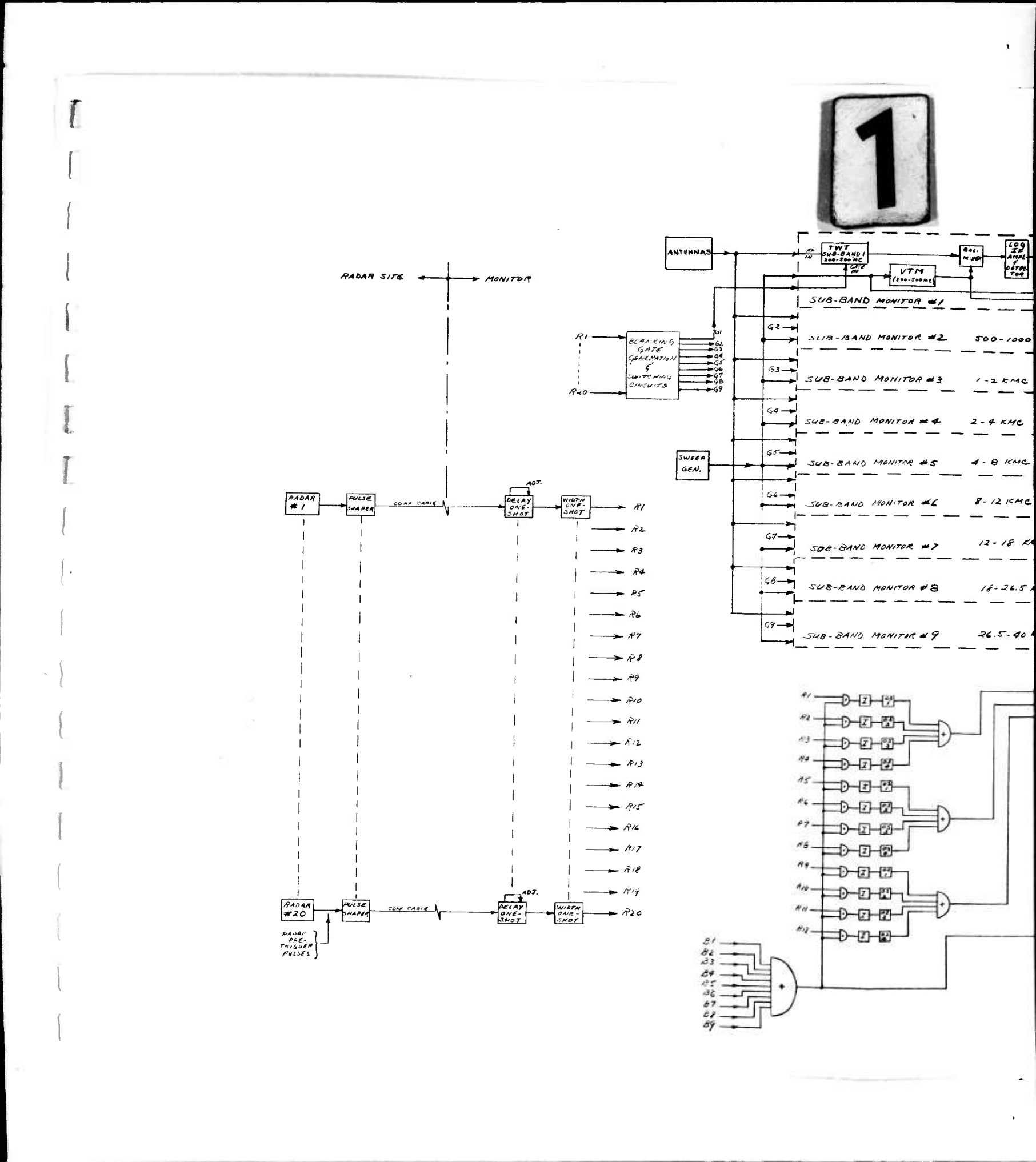
1
RADAR SITE
MONITOR
ANTENNAS
TWT SUB-BAND I 200-500 MC
VTM (200-500 MC)
SUB-BAND MONITOR #1
SUB-BAND MONITOR #2
500-1000
SUB-BAND MONITOR #3
1-2 KMC
SUB-BAND MONITOR #4
2-4 KMC
SUB-BAND MONITOR #5
4-8 KMC
SUB-BAND MONITOR #6
8-12 KMC
SUB-BAND MONITOR #7
SUB-BAND MONITOR #8
SUB-BAND MONITOR #9
SWEEP GEN.
BLANKING GATE GENERATION & SWITCHING CIRCUITS
R1
R20
G1
G2
G3
G4
G5
G6
G7
G8
G9
RADAR #1
PULSE SHAPER
COAX CABLE
DELAY ONE-SHOT
ADJ.
WIDTH ONE-SHOT
R1
R2
R3
R4
R5
R6
R7
R8
R9
R10
R11
R12
R13
R14
R15
R16
R17
R18
R19
R20
RADAR #20
RADAR PRE-TRIGGER PULSES
B1
B2
B3
B4
B5
B6
B7
B8
B9

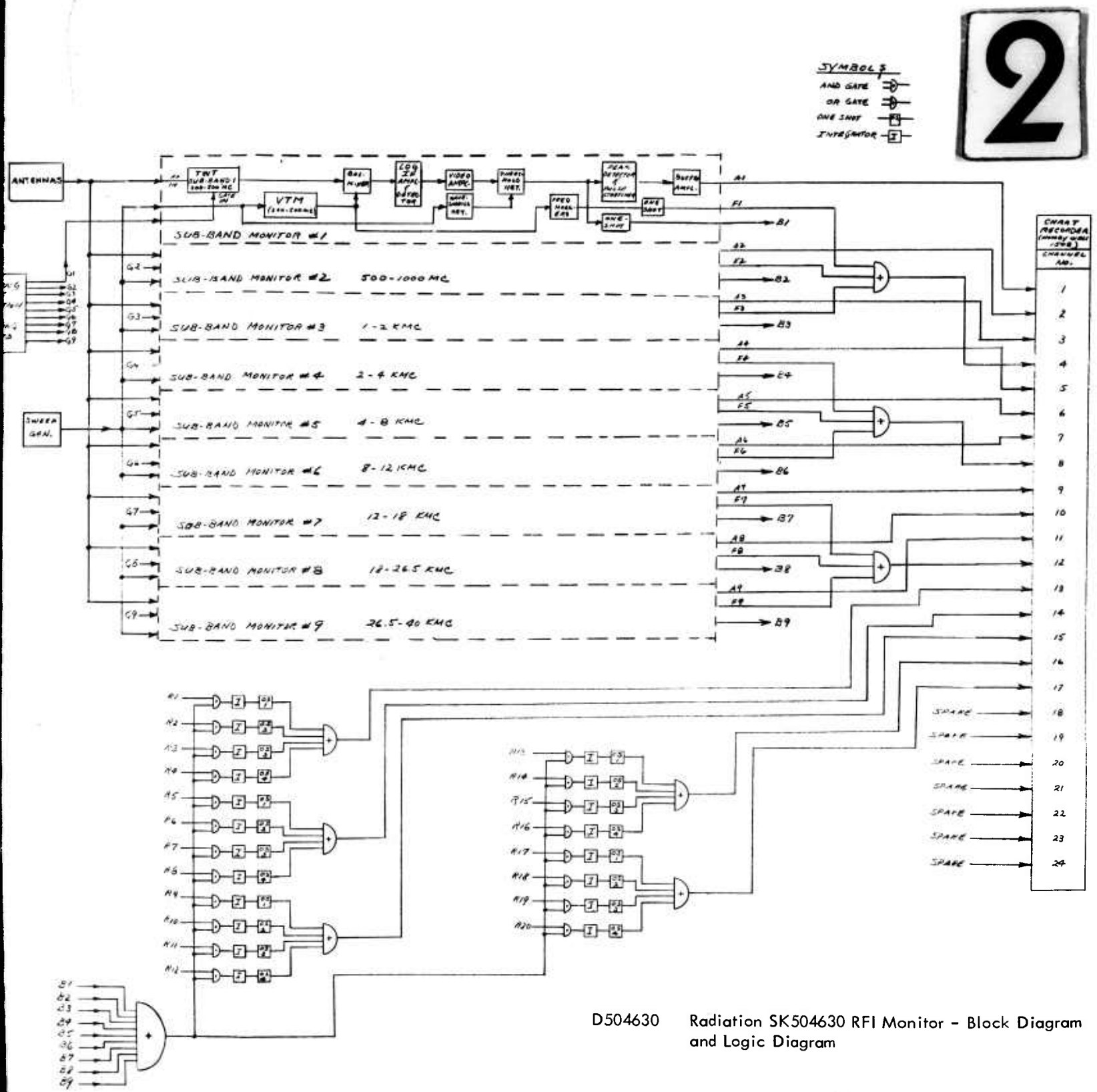

D504630 Radiation SK504630 RFI Monitor - Block Diagram and Logic Diagram